Vitrification a versatile method to modulate properties of myrcene-based rubbers

Farhad Asempour [a], Milan Maric [a,b] *

[a] Department of Chemical Engineering, McGill University, 3610 University St, Montreal, H3A 0C5, Quebec, Canada

[b] McGill Institute of Advanced Materials (MIAM), Quebec Centre for Advanced Materials (CQMF / QCAM), Canada

* Corresponding author

E-mail address: milan.maric@mcgill.ca

Keywords: bio-based elastomer, recyclable, terpene, vinylogous urethane, dynamic cross-linking, shape memory, nitroxide mediated polymerization

Graphical abstract

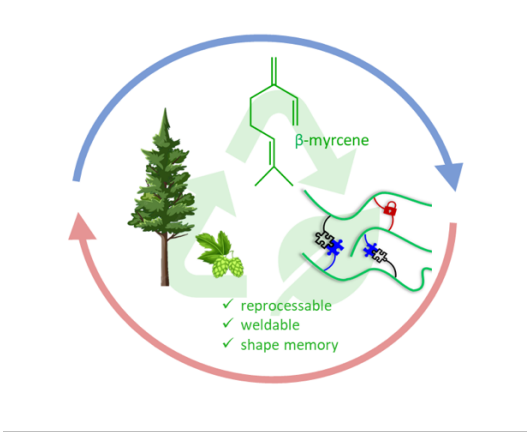

Abstract

We report bio-derived vitrimeric rubbers with weldability and excellent reprocessability. Reversible deactivation radical copolymerization of the commercially available terpene-based β-myrcene with 10 to 30 mol% (2-acetoacetoxy)ethyl methacrylate (AAEMA) afforded linear prepolymers which were cross-linked in a single step treatment with difunctional amine, the vegetable oil-derived Priamine 1075, or trifunctional amine tris(2-aminoethyl)amine (TREN). Decoupling the networks' backbone structure and cross-linkers led to high tunability of the vitrimers' final mechanical and rheological properties using prepolymer composition, molecular weight, nature and concentration of cross-linker and cross-linking density. Glass transition temperature (T_g) of the vitrimers ranged between -49 to -5 °C while the average elongation and stress at break ranged from ~83% and 0.18 MPa to ~30% and 1.68 MPa respectively from the lowest, 0.12 mol/L, to the highest, 0.98 mol/L, cross-linking densities. Characteristic features of dynamic vinylogous urethane-vitrimers were confirmed over at least 3 reprocessing cycles by grounding and hot pressing at 110 °C. No appreciable change in the ATR-FTIR spectra, T_g, decomposition temperatures, tensile properties and storage modulus were observed due to the reprocessing. Furthermore, incorporation of 5 mol% epoxy-based glycidyl methacrylate into the prepolymer led to the formation of a network with dual static and dynamic cross-links. Compared to the counterpart network with solely dynamic cross-links, the addition of static cross-links decreased creep by 75% and imparted shape memory effects. This work shows that combining vitrimer chemistry with myrcene is a facile and inexpensive, yet highly versatile method to not only modulate and compensate for the poorer mechanical properties of brush-like terpene-based elastomers but also provides a potential platform for recyclable bio-based rubbers with more sophisticated functionalities.

1. Introduction

Global warming and plastic waste pollution are considered planetary threats [1]. As a result, there is a growing interest in shifting from petroleum-based single-use polymers towards renewably sourced plastics with improved recyclability [2,3]. In this work, we are particularly focusing on the development of "greener" alternatives for thermosetting elastomers. Given the massive size of the synthetic rubber industry, with the current estimation of 15 to 20 million metric tons (MMT) per year, even small improvements can have significant environmental benefits [4,5].

Thermosets and elastomers are an irreplaceable category of polymers with substantial advantages associated with their mechanical, thermal, and chemical resistant properties [6]. However, due to their cross-linked molecular structure, they are commonly difficult to (re)process and recycle [7,8]. This issue has historically drawn a lot of attention from the polymer community. In the past two decades, covalent adaptable networks (CANs) exhibiting reversible covalent chemistry have appeared to offer a possible solution [9–12]. However, CANs can undergo depolymerization under certain conditions and temperatures, limiting their applications [5]. This has led to the development of vitrimers, first reported in 2011, as a new category of polymeric materials bridging the gap between thermosets and thermoplastics [5,13,14]. Vitrimers are permanently cross-linked networks with thermally induced "associative" dynamic covalent bonds [15,16]. This provides them with a unique ability to behave like thermosets at service temperatures but can change topology and be reprocessed without decreasing connectivity and dissolution at elevated temperatures [6,17]. Several catalyst-free chemistries such as exchanges of silyl ethers [18,19], imines [20,21], vinylogous urethanes [6,22,23], disulfides [5,24], dioxaborolane metathesis [17,25–27], hydroxy urethanes [28] and metathesis of cyclic acetals [29] have been reported, showing great potential for malleability, shape memory, and weldability [30–34]. Despite these advantageous properties, it has been commonly reported that

vitrimers undergo substantially higher creep compared to their static thermosetting counterparts [6,35]. Improving the dimensional stability of vitrimers is still an evolving area of research. It has been shown that a vitrimer's molecular architecture greatly influences its malleability and rheological properties [36–38].

In addition to reprocessability and recyclability, renewability plays a key role in the development of more sustainable polymeric materials [39]. Aside from natural rubber, various bio-based platforms such as itaconic acids, vegetable oils, lactides, norbornenes, and terpenes have shown much potential to produce rubbers [39,40]. Terpenes are particularly promising candidates as they can undergo radical polymerization with comparatively higher efficiencies [40–42]. Terpenes are made from highly abundant forestry feedstocks and are composed essentially of isoprenic motifs. Specifically, β-Myrcene (Myr) is a readily available acyclic monoterpene with a conjugated diene structure[43]. Myr can be isolated from pine, hops, bay leaves, lemongrass, celery, nutmeg, and rosemary [44,45]. Myr is industrially produced by pyrolysis of β-pinene, a major constituent of natural turpentine oil [45]. Similar to other 1,3-dienes, such as butadiene and isoprene, poly(Myr) also forms low glass transition temperature (T_g) (~ -75 °C) rubbery polymers [46]. In addition to renewability, an advantage of Myr over butadiene and isoprene is its lower volatility with a boiling point of 167 °C, meaning that Myr does not require pressurized equipment to handle [47]. However, the longer pendent side chain in poly(Myr) results in a higher entanglement molecular weight of ~ 18 kg/mol compared to that of poly(butadiene) and poly(isoprene) with ~ 3 and ~6 kg/mol respectively [46,48]. This in general can result in lower tensile strength, elongation, and toughness of poly(Myr), potentially limiting its applications [43,49]. Although some in-depth studies involving various polymerization techniques and properties of poly(Myr) have been reported, thorough investigations on the applications of poly(Myr)-based elastomers in the rubber industry are

generally lacking in the literature [48,50,51]. Some works have investigated applications of vulcanized poly(Myr) as well as Myr-based thermoplastic elastomers with styrene and isobornyl methacrylate (IBOMA)[47,52–55]. Bhowmick's and Gong's groups have also reported Myr-based CANs using Diels-Alder chemistry via Myr copolymerizations with furan-based monomers. The resulting elastomers exhibited self-healing and shape memory properties [56,57].

Recently several works have reported promising results combining renewability and recyclability via vitrimer chemistry to produce elastomers [58]. Kolsch et al. synthesized poly(itaconate) elastomers with catalytic transesterification [59]. Feng et al. prepared photothermally induced self-healable and shape memory epoxidized natural rubber-based elastomers using catalytic transesterification [60]. Liu et al. reported the development of a cross-linker with triple dynamic covalent bonds (boroxine, disulfide bond, imine bond) for the vitrification of epoxidized natural rubber, imparting self-healing and recyclability [61].

In this study, we report a facile method to produce thermally reprocessable bio-derived vitrimeric rubbers based on catalyst-free vinylogous urethane exchanges. Well-defined copolymers of inexpensive and commercially available Myr with a monomer containing a reactive β-ketoester moiety, 2-acetoacetoxy)ethyl methacrylate (AAEMA), were synthesized using nitroxide mediated polymerization (NMP). Two different cross-linkers, Priamine 1075 (referred to simply as Priamine hereafter), a long-chain dimer diamine with 100% bio-based carbon content, as well as tris(2-aminoethyl)amine (TREN), a smaller triamine molecule, were utilized to tailor cross-linking density. Thermomechanical tests showed that the resulting vitrimers had excellent reprocessability after three cycles of grounding and hot pressing. Moreover, to suppress creep and eventually impart shape memory effects, terpolymers of Myr, AAEMA, and glycidyl methacrylate (GMA), the latter containing an epoxy moiety, were synthesized. Upon reactions with amines, a dual static

and dynamic network was formed. The use of different prepolymer compositions, cross-linkers, and the addition of the low number of static cross-links provided a versatile toolbox to tune the final mechanical and rheological properties of the vitrimers.

2. Experimental

2.1. Materials

All chemicals were of reagent grade and used as received unless otherwise stated. β-Myrcene (Myr, Sigma-Aldrich, ≥90%), (2-acetoacetoxy)ethyl methacrylate (AAEMA, TCI, 95%), glycidyl methacrylate (GMA, Sigma-Aldrich, 97%) were purified by passing through columns of basic alumina (Al_2O_3, Brockmann, Type I, Sigma-Aldrich) mixed with 5 wt% calcium hydride (90-95%, Sigma-Aldrich) and stored in a refrigerator under a head of nitrogen until needed. Priamine 1075 (Priamine) was procured from Cargill and tris(2-aminoethyl)amine (TREN, 97%) was purchased from Alfa Aesar. Butylamine (99%) was purchased from Sigma-Aldrich. Tetrahydrofuran (THF, HPLC grade), toluene (>99%), chloroform (>99%), N,N- dimethylformamide (DMF, >99%), acetone (>99%), reagent alcohol (anhydrous ethanol 90% v/v; methanol 5% v/v; 2-Propanol 5% v/v), methanol (>99%) were purchased from Fisher Scientific. Deuterated chloroform ($CDCl_3$, ≥99%) was purchased from Cambridge Isotopes Laboratory for ^1H NMR analyses.

BlocBuilder ™ (BB, also known as MAMA-SG1, is the alkoxyamine for NMP, and SG1 is the free nitroxide, see Figure S1 for more details) was obtained from Arkema. 2-Methyl-2-[N-tert-butyl-N-(1-diethoxyphosphoryl-2,2-dimethylpropyl)-aminoxy]–N-propionyloxy-succinimide (NHS-BB, also known as NHS-BlocBuilder) was synthesized according to the previous literature [62]. N,N'-dicyclohexylcarbodiimide (DCC), N-hydroxysuccinimide (NHS) were procured from Sigma Aldrich.

2.2. Polymer synthesis

We synthesized three different statistical copolymers of Myr with either 10, 20, or 30 mol% AAEMA content with similar molecular weights. NMP with BlocBuilder, an SG1-based alkoxyamine, was used to initiate and control the synthesis of well-defined prepolymers. All polymerizations were performed in bulk. Table 1 summarizes the copolymerization formulae and reaction conditions for prepolymers. As an example, for the synthesis of MyrAA-20 prepolymer, Myr (56.45 g, 414.3 mmol), AAEMA (22.2 g, 103.6 mmol), BlocBuilder (1.2 g, 3.145mmol), and a magnetic stir bar were added to a 250 mL three-neck round-bottom glass flask. The reactor was equipped with an overhead reflux condenser connected to a chiller (Fisher Scientific Isotemp 3016D) at 2 ˚C. The reaction solution was sparged with high-purity N_2 gas for 20-25 minutes prior to being heated at 125 ˚C for 8h using a heating mantle and a feedback temperature controller. Samples were periodically taken for ^{1}H NMR and GPC analyses. Afterward, the reaction was stopped by lowering the temperature, and the obtained viscous solution was three times (re)precipitated into a mixture of ethanol/methanol (70/30 v/v%) from THF. It should be noted that, the (re)precipitation and work up resulted in some polymer loss. Finally, the polymer was dried under a reduced pressure at 60 ˚C overnight, yielding 39.1 g of a yellow-colored viscous liquid. The overall monomer conversion from ^{1}H NMR was 88.2%, see Supporting Information section S2, and from gel permeation chromatography (GPC), the number average molecular weight (M_n) was 12,800 g/mol with the dispersity ($Đ$) of 1.49 relative to PMMA standards.

We also studied the effects of physical molecular entanglements on the rheological properties of vitrimers. To do so, we synthesized a prepolymer with a molecular weight higher than the entanglement molecular weight (M_e) of poly(Myr) homopolymer, MyrAA-30-Long, by increasing the theoretical target molecular weight to 60 000 g/mol at 100% monomer conversion.

Furthermore, to incorporate static cross-links into the vitrimeric network, we prepared a terpolymer of Myr with 20 mol% AAEMA and 5 mol% GMA. For the synthesis of the GMA-bearing prepolymer, a different initiator with an SG1-based alkoxyamine initiator bearing an N-succinimidyl ester group was synthesized (NHS-BlocBuilder) and utilized according to the literature [63].

The prepolymers are coded as MyrAA-xx, where xx refers to the AAEMA mol% in the initial monomer mixture composition. The high molecular weight polymer was coded as MyrAA-30-Long, and the copolymer with 5 mol% GMA content was named MyrAA-20-GMA-5.

Table 1. Myrcene/ AAEMA/ GMA copolymerization formulae and synthesis conditions

prepolymer code [a]	$[Alkoxyamine]_0$ (M) [c]	$[Myr]_0$ (M) [d]	$[AAEMA]_0$ (M)	$[GMA]_0$ (M)	$M_{n,\,target}$ [e] (g/mol)	T (˚C)	time (h)
MyrAA-10 [a]	0.033	5.19	0.58	—	25,000	125	8.5
MyrAA-20 [a]	0.035	4.56	1.21	—	25,000	125	8
MyrAA-30 [a]	0.036	3.82	1.79	—	25,000	125	6
MyrAA-30-Long [b]	0.015	3.83	1.79	—	60,000	125	8
MyrAA-20-GMA-5	0.033	4.32	1.15	0.29	25,000	125	6

[a] Experimental identification of copolymers: MyrAA-xx, where xx referees to the initial molar ratio of AAEMA

[b] Long refers to prepolymer with higher target number average molecular weight (M_n)

[c] Molar concentration of BlocBuilder, or NHS-BlocBuilder in case of MyrAA-20-GMA-5

[d] Initial monomer molar concentration in the feed

[e] Target M_n at 100% conversion

2.3. Formation of vitrimers and (re)processing

Vitrification of a prepolymer started with dissolving it in THF, 40% (w/v), followed by the addition of either Priamine or TREN and stirring until gelation. The resulting gel was left overnight at room temperature in a fume hood and was further cured and dried at 75 ± 10˚C under reduced pressure in a vacuum oven for 8-12 h. The resulting vitrimer was ground up and hot pressed (Carver Manual Hydraulic Press with Watlow temperature controllers), while sandwiched between two Teflon

plates, at 110 ± 5 ˚C under 6 ± 1 metric tons for 50 ± 5 min yielding a yellow and transparent shaped material. See Supporting Information and Figure S3 for each step. To further explore the effects of cross-linking density, two different ratios of β-ketoester : amine were studied; 1:1 and 0.7:1. Vitrified polymers are coded as "MyrAA-xx-P/T-yy" where xx is the rounded molar ratio of the AAEMA, P/T shows the type of cross-linker, T for TREN or P for Priamine, and yy indicates the molar ratio of β-ketoesters from AAEMA in the co/terpolymer to NH_2 from the cross-linker. As an example, *MyrAA-20-T-0.7* represents a vitrified polymer with 20 mol% AAEMA which is cross-linked with TREN with a 0.7:1 ratio of β-ketoesters to NH_2.

2.4.Characterization

Nuclear Magnetic Resonance (NMR) Spectroscopy

^{1}H NMR spectra were recorded on a Bruker AVIIIHD 500 MHz Spectrometer using 16 scans with $CDCl_3$ at room temperature.

Gel Permeation Chromatography (GPC)

The number average molecular weight (M_n) and dispersity ($Đ = M_w/ M_n$) of the polymers synthesized were estimated using GPC (Waters, Breeze System) in THF (HPLC) at 40 °C and a flow rate of 0.3 mL/min. The GPC system was equipped with a guard column, a differential refractive index (RI 2414) detector and three Styragel HR columns (with a molecular weight measurement range of 10^2 to 5×10^3 g/mol for HR1, 5×10^2 to 2×10^4 g/mol for HR2 and 5×10^3 to 6×10^5 g/mol for HR4). Poly(methyl methacrylate) (PMMA) (Varian) standards were used for calibration of molecular weights ranging from 875 to 1,677,000 g/mol.

FT-IR Spectroscopy

Infrared spectra were collected on a Thermo Scientific Nicolet™ iS50 FTIR Spectrometer equipped with diamond attenuated total reflectance (ATR) accessory using 32 scans.

Differential Scanning Calorimetry (DSC)

DSC experiments were collected on a Discovery 2500 TA Instruments equipped with an autosampler and refrigerated cooling system (RSC 90) using aluminum hermetic pin-hole pans. Calibrations for temperature and heat flow were carried out using indium and benzoic acid standards. Temperature ramp experiments (cool/heat/cool/heat) were run from -90 to 30 °C under nitrogen with heating rate of 15 °C/min and cooling rate of 10 °C/min with 3-min isotherms at each extreme. Experimental data were recorded and analyzed using TA instrument TRIOS software. The reported T_g were calculated using the curve inflection and only the second heating run was considered to remove any thermal history.

Thermal Gravimetric Analysis (TGA)

To study the thermal stability of the polymers, a TA Instrument's Discovery TGA 5500 with autosampler and platinum pans were used. All experiments were done under a nitrogen flow. The samples were heated to 100 °C for 30 min isotherms prior to each run to remove any moisture or residual solvent. Ramp experiments were performed with a heating rate of 15 °C/min until 650 °C. Isothermal experiments were done from room temperature up to 110 °C and remained at the temperature for a 6 h total run time.

Tensile Analysis Testing

Tests were performed on a universal Shimadzu Easy Test system with a 500 N load cell and a crosshead speed of 10 mm/min. Dog-bone shaped tensile specimen similar to ASTM D638 type V (overall length of 60 mm and respective neck thickness and width of approximately 2 and 3mm) were prepared using a Carver hot-press as described previously[23]. Reported results are the average of at least 3 specimens.

Dynamic Mechanical Analysis (DMA) and Rheology

All tests were done using an Anton Paar MCR 302. DMA tests were conducted using a solid rectangular fixture (SFR 12). Rectangular-shaped samples (60mm length, 10mm width, and 2mm thickness) were heated from room temperature to 130 °C with an average rate of 5 °C/min and at a frequency of 1 Hz. Rheological tests were done with a 25 mm parallel plates geometry. Strain sweep tests were carried out at 100-130 °C to determine the linear viscoelastic region (LVR) at 1 Hz. Stress relaxation experiments were conducted at 0.1 % strain at the desired temperatures. Creep recovery experiments were performed at 1000 Pa for 300 s followed by 0 Pa for 600 s, for a total experiment time of 900 s.

Gel fraction and swelling tests

Gel fraction was obtained by soaking the networks in excess amount of a desired solvent for 72 hours at room temperature. Next, the swelled samples were filtered, dabbed with delicate task wipes to remove any excess solvent, and immediately weighed to find the samples' swelling ratio. This was followed by drying the samples in a vacuum oven at reduced pressure and 60 °C for a day, and finally weighing them. Gel fraction was calculated using m_2 / m_0 where m_0 is the original mass of the sample and m_2 is the mass of dried sample after swelling.

3. Results and discussion

3.1. prepolymer synthesis and characterization

We anticipated that the thermomechanical properties of the final vitrimers would be dictated by those of the linear reactive precursors. Therefore, we commenced our studies by synthesizing statistical copolymers of Myr with AAEMA, which provides the functionality for amine-crosslinking. NMP with BlocBuilder was used to control the molecular weight of the prepolymers and minimize possible side reactions and cross-linking of Myr during the polymerization.

Copolymerizations of Myr using reversible-deactivation radical polymerization (RDRP) have been reported [40,42,64]. For example, Pablo-Morales et al. and Hilschman et al. utilized reversible addition−fragmentation chain-transfer (RAFT) for copolymerization of Myr with GMA and styrene respectively [65,66]. Métafiot et al. showed effective copolymerization of Myr with methacrylates such as IBOMA and GMA with highly regioregular microstructure using NMP[47,52,67]. Herein, NMP was adopted since it does not rely on sulfur-based chain transfer agents or any metallic ligands [68–70]. This is particularly important since the thiocarbonylthio chain transfer agent moieties in RAFT are prone to rapid aminolysis upon treatment with primary amines and therefore chain end modification is required before further processing [23,34].

Three different prepolymers with initial AAEMA feed ratios of 10, 20 and 30 mol% were prepared to investigate the effects of cross-linking density. See Figure 1 and S1 for the synthetic route used to prepare these copolymers. Table 2 summarizes the overall monomer conversion, molecular and thermal characterization of all synthesized prepolymers. Characterization by GPC showed that the M_n of the MyrAA-10, 20 and 30 were predictable, ranging from 11.8 to 12.8 kg/mol with relatively low dispersities ($Đ$) of 1.38 to 1.51. It should be mentioned that some deviation from the theoretical M_n was observed which indicates divergence from the ideal persistent radical effect and the possibility of chain transfer and/or termination reactions [68,71]. Additionally, all M_ns reported were relative to PMMA standards, which may introduce some error as the copolymers were largely Myr-based in composition. Figure 2 illustrates representative kinetic plots and molecular weight characterizations of MyrAA-10. From the ^{1}H NMR analyses, a pseudo-first-order linear monomer conversion over time was observed. Reasonable overall monomer conversion of 76 to 89% for Myr, and >95% for AAEMA were achieved. See Figures S4 and S5 for representative ^{1}H NMR spectra, calculations of conversion, and Figure S6 for GPC traces. The observed linear trend of

chain growth combined with the low $Đ$ suggest that the possible side reactions and chain terminations were largely suppressed [68,72]. Figure S7 shows the ratio of unreacted AAEMA to Myr monomers as a function of the polymerization time of MyrAA-10. A decrease in the reactants' composition ratio from 0.11 to 0.01 over time suggests some compositional drift in the prepolymers. Further investigation on the reactivity ratios and compositional drift of Myr and AAEMA is underway and will be addressed separately. Via ^{1}H NMR, the microstructure of the incorporated Myr was also determined. Myr can be polymerized into 3 different regioisomers: 1,4-, 3,4- and 1,2- vinyl addition [47,53]. All prepolymers had high regioregularity with >90% of the 1, 4-addition structure, which agrees with the literature [49,53,65].

In the second part of our study, we aimed to suppress creep in the vitrimers using two strategies: incorporating physical chain entanglements or adding chemically static cross-links. To achieve the first strategy, we synthesized a statistical prepolymer of Myr and AAEMA with M_n of 22 kg/mol (coded as MyrAA-30-Long) which is slightly higher than the critical entanglement molecular weight (M_e) of poly(Myr) homopolymer (M_e ~18 kg/mol) [46,73]. Figure S8 shows the GPC traces of all prepolymers. A clear shift towards higher molecular weights was observed for MyrAA-30-Long.

Moreover, we incorporated GMA in MyrAA-20-GMA-5 prepolymer, as seen in Figure 1. The epoxy group in GMA can react with amines and generate secondary chemically static cross-links. For the synthesis of the GMA-based prepolymer we used NHS-BlocBuilder instead of neat BlocBuilder. This was to avoid side reactions between the epoxy group and carboxylic acid groups from BlocBuilder [63,67]. Interestingly, MyrAA-20-GMA-5 had a comparatively lower $Đ$ of 1.29. This can be attributed to a higher dissociation rate and slightly lower activation energy of NHS-BlocBuilder, compared to BlocBuilder, which mimics the use of additional controlling SG1,

thereby providing more efficient control [62,67]. Incorporation of epoxy groups was confirmed by ^{1}H NMR, Figure S5.

From the DSC traces, T_g of the prepolymers systematically increased from -63 °C to -49 °C by increasing the AAEMA and GMA content; see Figure S9 for the DSC experiments. The measured T_gs are in good agreement with the estimates from the Flory-Fox equation [74], see Table S1 for the details.

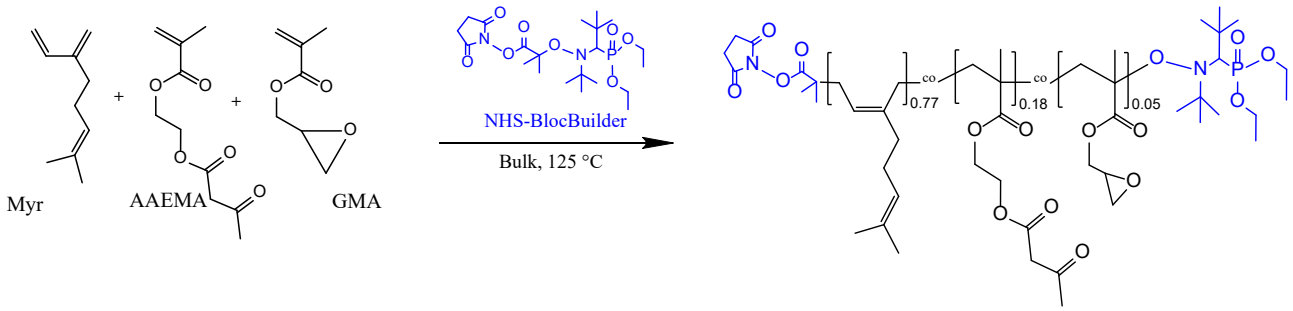

Figure 1. Statistical copolymerization of MyrAA-20-GMA-5 with NHS-BlocBuilder. A controlled radical polymerization was achieved using NMP.

Table 2. Molecular and thermal characterizations for various synthesized prepolymers

code	X (%) [a]	*Mn* (g/mol) b	*Đ* b	F $_{Myr}$ [c]	1,4 addition	F $_{AAEMA}$	F $_{GMA}$	*Tg* (°C) d
MyrAA-10	70.0%	11,800	1.38	90%	93.5%	10%	—	-63
MyrAA-20	88.2%	12,750	1.49	82%	89.6%	18%	—	-62
MyrAA-30	92.6%	12,650	1.51	69%	93.6%	31%	—	-53
MyrAA-30-Long	90.2%	22,060	1.45	70%	92.3%	30%	—	-54
MyrAA-20-GMA-5	79.5%	13,860	1.29	77%	92.4%	18%	5%	-49

[a] Overall monomer conversion determined by ^{1}H NMR
[b] Number average molecular weight (M_n) and dispersity ($Đ$) from GPC relative to PMMA standard in THF at 40 ˚C
[c] Molar fraction of monomers in the final polymer determined by ^{1}H NMR
[d] Percentage of 1,4 addition microstructure in poly(Myr)
[e] Determined by DSC

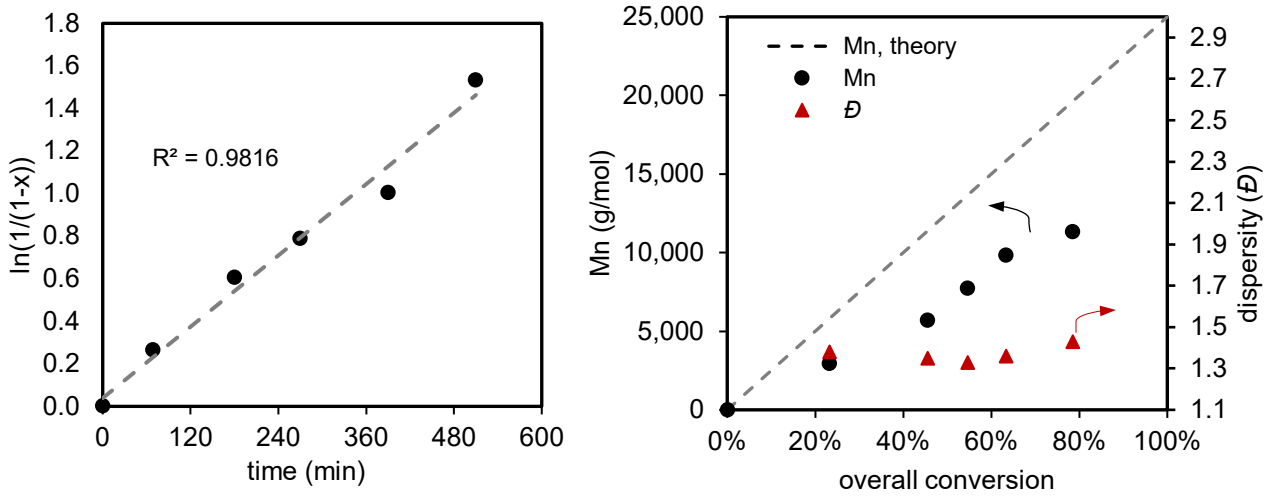

Figure 2. Representative polymerization data of MyrAA-10 prepolymer: left) linearized overall monomer conversion versus time and right) evolution of M_n and $Đ$ against overall monomer conversion.

3.2. Vitrimer network synthesis and characterization

Once the prepolymers were prepared, vitrification was performed by simple solution casting, as seen in Figure S3. Two different cross-linkers were used. TREN, a small trifunctional molecule and Priamine, a difunctional vegetable oil-based molecule with relatively longer arms, are shown in Figure 3. Due to the associative nature of transamination, a stoichiometric imbalance is required to have an effective cross-linking exchange [13,23,34,75]. However, the effects of cross-linking ratio on the rheological properties and dimensional stability of vitrimers have generally been limited [6,34, 38, 76]. Therefore, we prepared networks with two different ratios of amine to β-ketoester for each cross-linking system to test for sensitivity. We were able to study the mechanical and rheological properties of the resulting vitrimers over a wide range of cross-linking densities by decoupling the structure and composition of the prepolymers from the nature and ratio of the cross-linkers.

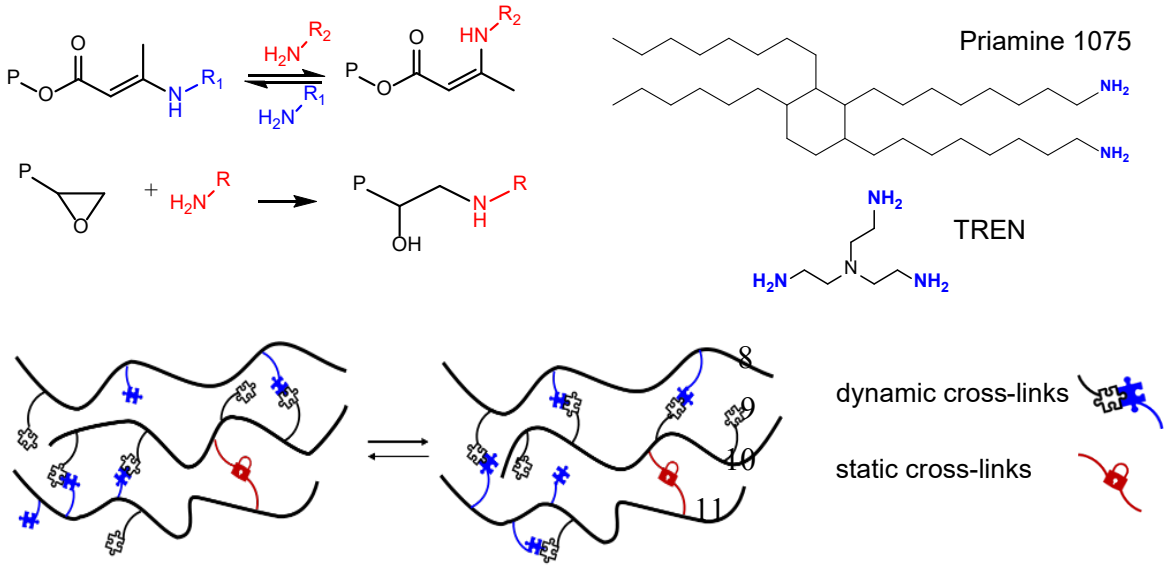

Figure 3. Cross-linking of MyrAA-20-GMA-5 prepolymer with Priamine or TREN. Both dynamic and static cross-links are present, enabling exchange and incorporation of shape memory behaviour.

3.3. Swelling test

Due to the associative nature of the reversible cross-links in vitrimers, the networks do not dissolve in solvents but swell [17,37,77,78]. Indeed, this was evident for all synthesized vitrimers. The results of swelling tests for various networks and solvents are summarized in Table 3. A compromise between the gel content and swelling ratio was observed. Swelling ratio increased with looser networks by shifting from TREN to Priamine. Expectedly, MyrAA-30-T-1, with the tightest network, had the lowest swelling ratio while MyrAA-10-P-0.7 exhibited the highest one, as it had the lowest β-ketoester concentration and higher free amine chain ends (β-ketoester/NH_2 = 0.7). Also, MyrAA-20-GMA-5-P-0.7 showed an intermediate value of cross-linking density between MyrAA-20-P-0.7 and MyrAA-30-P-0.7 as expected.

Table 3. Swelling results of various vitrimers in toluene and gel content of MyrAA-20-T-0.7 in THF

Vitrimer	**MyrAA-30 -T-1**	**MyrAA-30 -T-0.7**	**MyrAA-30 -P-1**	**MyrAA-30 -P-0.7**	**MyrAA-20 - P-0.7**	**MyrAA-10 -P-0.7**	**MyrAA-20-GMA-5 -P-0.7**
Gel Content*	95%	95%	95%	93%	91%	87%	96%
Swelling ratio*	202%	235%	242%	261%	361%	692%	294%
Solvent	THF	Toluene	Chloroform	DMF	Methanol		
Gel Content**	92%	89%	91%	93%	93%		

* in toluene

** Tests done with MyrAA-20-T-0.7

The cross-link densities (υ_e) of equilibrated swollen networks were estimated using the Flory-Rehner equation (eq 1):

$$\upsilon_e = -\frac{ln(1-V_r)+V_r+\chi_{12}\,V_r^2}{V_s\left(V_r^{\frac{1}{3}}-\frac{V_r}{2}\right)} \qquad \text{(eq 1)}$$

in which V_s is the molar volume of solvent (106.5 cm^3/mol for toluene[79]) and V_r is the volume fraction of polymer network in the swollen sample, calculated using equation 2) [80,81]. χ_{12} is the Flory-Huggins polymer-solvent interaction parameter and is estimated using the Flory-Hildebrand equation (eq. 3)[81].

$$V_r = \frac{\frac{m_2}{\rho_2}}{\frac{m_1}{\rho_1}+\frac{m_2}{\rho_2}} \qquad \text{(eq 2)}$$

$$\chi_{12} = \frac{V_s}{RT}\,(\delta_s - \delta_p)^2 \qquad \text{(eq 3)}$$

Here, m_1 and m_2 are the mass of the swollen and vacuum dried samples and δ_s and δ_p are the solubility parameters of the solvent and polymer [55,82]. δ_p of different prepolymers were either taken from the literature or estimated using the group contribution method of Hoftyzer and van Krevelen with a weighted average of different comonomers using the volume fraction[67,83]. See section S5 in the Supporting Information for the details of calculations. Figure 4 compares the cross-linking density of the various networks studied ranging between the two extremes. As expected, the sample with highest AAEMA content and a balanced β-ketoester : amine ratio exhibited the

highest cross-linking density of 0.98 mol/L. In contrast, MyrAA-10-P-0.7 which had the lowest AAEMA content and was cross-linked with excess Priamine expectedly showed lowest cross-linking density of 0.12 mol/L. This trend correlates with the results from the DSC analyses and the shift in the T_gs of the vitrimers discussed in section 2.4.

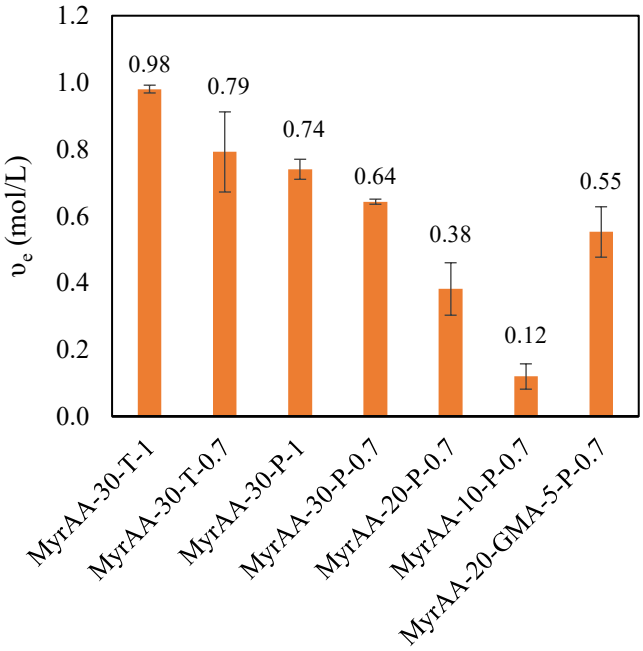

Figure 4. Comparisons of the cross-link density of various networks from highest to lowest, calculated using the Flory-Rehner equation and swelling tests in toluene. A monotonic rise in cross-linking density was observed with increasing AAEMA content and balancing the stoichiometric cross-linking ratio.

Network disintegration and polymer recovery

Considering the dynamic nature of transamination in vinylogous urethanes, we hypothesized that by adding an excess amount of a monofunctional amine, the network can be disintegrated, and the prepolymer be chemically recovered [23,84]. Thus, MyrAA-20-P-0.7 with toluene and excess butylamine were added to a vial and sealed. Interestingly, the network did not dissolve after 24hr at room temperature; however, once the vial was placed in an oven at 110 ± 5 °C the vitrimer was

fully dissolved in a few hours. Figure 5 and Table 4 compare the GPC traces and molecular weights of MyrAA-20 prepolymer and MyrAA-20-P-0.7 after disintegration and chemical recovery. These results confirm that the vitrimer processing, shaping, and chemical recovery of the prepolymer did not significantly degrade the polymer backbone.

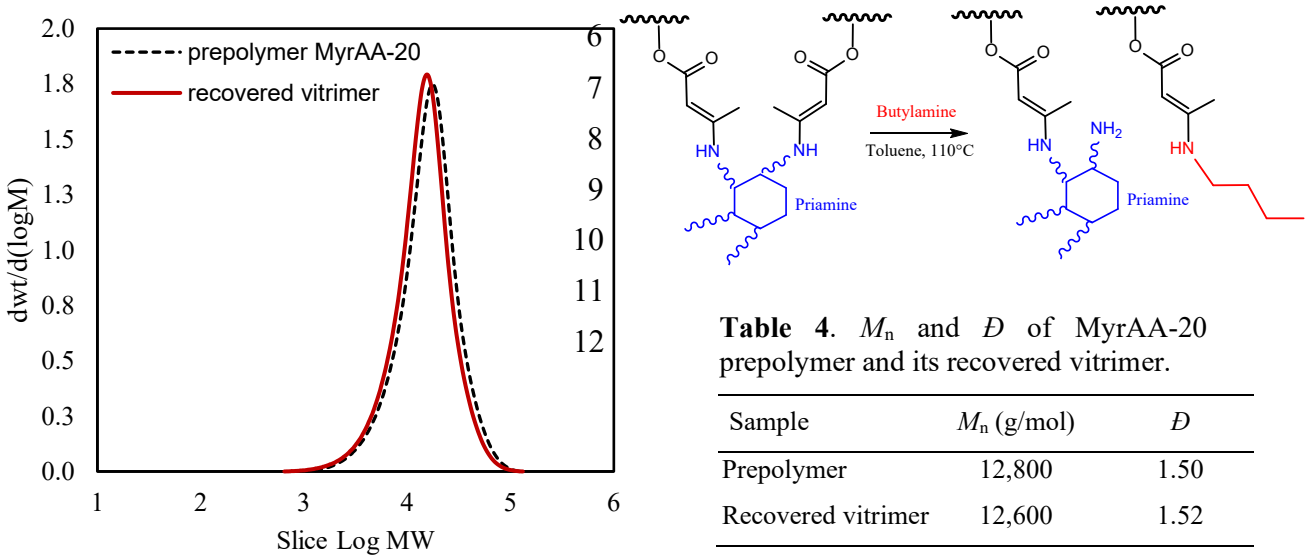

Table 4. M_n and $Đ$ of MyrAA-20 prepolymer and its recovered vitrimer.

Sample	M_n (g/mol)	$Đ$
Prepolymer	12,800	1.50
Recovered vitrimer	12,600	1.52

Figure 5. Schematic of vitrimer disintegration (right) and comparison of GPC traces of MyrAA-20 and its recovered vitrimer, MyrAA-20-P-0.7 (left) using butylamine.

3.4. Thermal and mechanical properties

The DSC traces of the MyrAA-30 prepolymer and its associated vitrimers are shown in Figure 6.a. A clear shift towards higher T_gs was observed after the network formation. Vitrimers cross-linked with TREN exhibited T_gs that were about 20 °C higher than those cross-linked with Priamine. This can be attributed to the higher cross-linking density of the TREN-based networks. However, it appears that changing the β-ketoester : amine ratios did not have a significant impact on the T_gs. Similar shift towards higher T_gs was observed for vitrified MyrAA-30-Long. Interestingly, although prepolymers of both MyrAA-30 and MyrAA-30-Long had similar T_gs, vitrified MyrAA-30-Long -T-0.7 had a T_g that was about 10 °C lower than that of the vitrified MyrAA-30-T-0.7.

One possible explanation for this is that there may have been a compositional drift in the prepolymers during the synthesis, resulting in the formation of longer Myr-rich sequences in the chains of MyrAA-30-Long, as seen in section 3.1 and Figure S7. Determination of reactivity ratios for this system is underway to verify if compositional drift is significant.

Figure 6.b illustrates the results of tensile tests performed with the various vitrimers. The tensile strength at break of the vitrimers systematically increased by increasing the AAEMA content in the copolymer. For samples cross-linked with excess difunctional amine (P-0.7), an increase in tensile strength from MyrAA-10-P-0.7 with 0.18 ± 0.03MPa to MyrAA-30-P-0.7 with 0.48 ± 0.03MPa was seen. Simultaneously, the opposite trend was observed for samples' elongation at break, as it decreased from 82.7 ± 18.6% for MyrAA-10-P.0.7 to 22.5±0.5% for MyrAA-20-P-0.7. In addition, The maximum tensile strength of 1.68 ± 0.02 MPa was observed for MyrAA-30-T-1. From Figure S19, it is evident that replacing the diamine cross-linker with the triamine one, resulted in the formation of stiffer materials in case of MyrAA-20-P-0.7 and MyrAA-20-T-0.7. A similar trend was observed by DMTA with a systematic increase in modulus from MyrAA-10-P-.07 to MyrAA-30-T-1. The tensile data closely follow the results of the swelling tests and cross-linking density calculations. These findings show that vitrification can be used as an effective tool to modulate the mechanical properties of terpene-based rubbers.

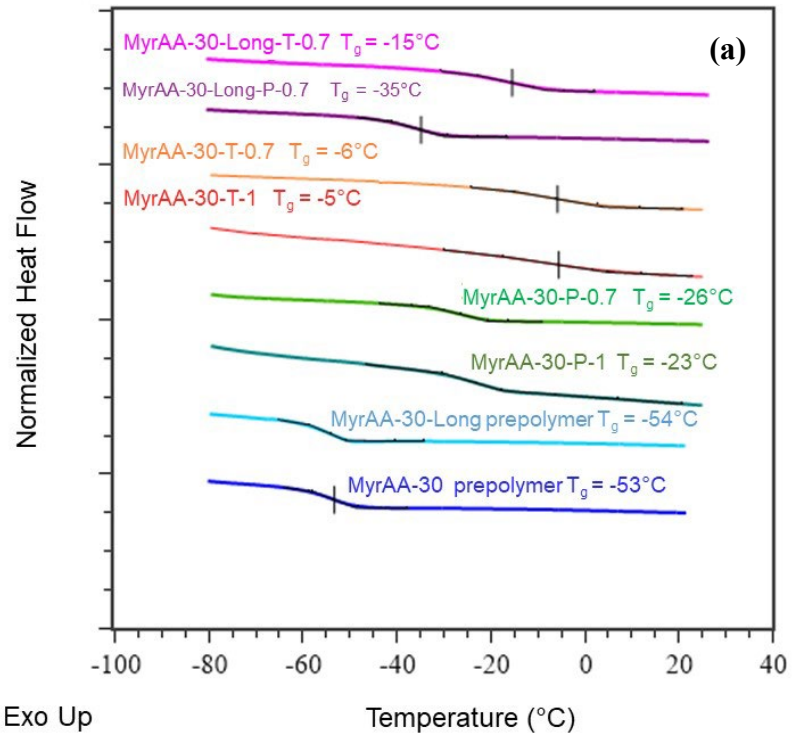

1

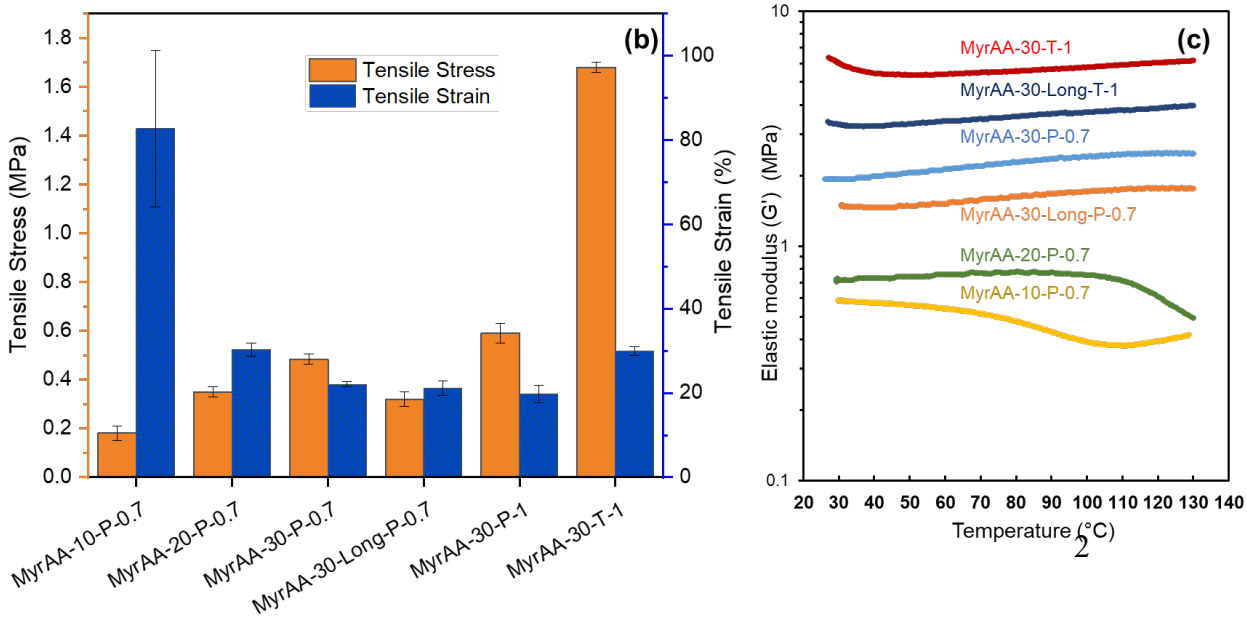

2

3

4 **Figure 6. a)** DSC traces of MyrAA-30 and MyrAA-30-Long prepolymer and their networks cross-
5 linked with two ratios of TREN and Priamine; vitrification increased the glass transition
6 temperature; **b)** Tensile data of various prepolymers cross-linked with Priamine with 0.7 to 1, and
7 TREN with 1:1 β-ketoester: amine ratios. Increasing the network cross-linking density
8 systematically reduced the elongation at break and increased tensile strength; **c)** representative
9 DMTA data, elastic modulus and rubbery plateau of the vitrimers increased with cross-linking
10 concentration.

3.5. Rheological properties

Stress-relaxation and creep

The recyclability of vitrimers is directly influenced by the exchange rate of the dynamic bonds due to their associative nature. The dynamic cross-link exchanges facilitate rearrangements in the network topology, segmental healing, and reformation of a continuous material macroscopically[13,37]. We carried out stress-relaxation experiments to investigate the flow behavior of the vitrimers and quantify the timescale of the conformational rearrangements. Figure 7 compares the normalized stress-relaxation spectra of various prepolymers vitrified with an excess amount of Priamine, P-0.7, at 130 °C. Increasing the AAEMA content systematically slowed down the stress-relaxation rate of the vitrimers which is in line with the networks' cross-linking density. Networks with 10 and 20 mol% AAEMA content showed fast and complete relaxation. Moreover, increasing the molecular weight of the prepolymer, in the case of MyrAA-30-Long-P, beyond the M_e, further slowed down the stress relaxation which suggests some restrictions in conformational rearrangements due to physical chain entanglements. Furthermore, addition of static cross-links via epoxy groups i.e., MyrAA-20-GMA-5, resulted in a significant increase of stress relaxation time with a portion of the stress never being fully relaxed after 1000 seconds.

Figure 8.a illustrates a typical normalized stress-relaxation i.e., G(t)/G(0), curve for MyrAA-30-T-0.7 in the temperature range of 90 to 130 °C. According to the single element Maxwell viscoelastic model, $G(t)/G(0) = -exp\ (t/\tau^*)$, the characteristic relaxation time (τ^*) is identified at the time when the normalized relaxation modulus reaches the value of e^{-1} (≈ 0.37) [85]. However, with increasing cross-linking density some deviations from the ideal Maxwellian behavior were observed. To capture these deviations, a stretched exponential decay model was

used according to equation 4. which permits the extraction of (τ*) for samples that do not fully relax past the e^{-1} point:

$$\frac{G\,(t)}{G\,(0)} = e^{-\left(\frac{t}{\tau^*}\right)^{\beta}} \qquad \text{(eq. 4)}$$

where, G(t) and G (0) are the relaxation moduli at time t and 0, τ^* is the characteristic relaxation time and β ($0 < \beta \leq 1$) is a parameter related to the breadth of the relaxation distribution. For MyrAA-30-T-0.7, β varies between 0.50 and 0.69 showing deviations from ideal Maxwellian behavior [6,16,85]. See Table S3 for detailed τ^* and β values obtained by curve-fitting. As suggested by Leibler et al., since a chemical reaction is responsible for the dynamic exchanges in cross-linking, an Arrhenius relationship can be used to model the gradual decrease of viscosity with increasing temperature according to equation 5 [6,74].

$$\ln \tau^* = \frac{E_a}{RT} + \ln\,(\tau_0) \qquad \text{(eq. 5)}$$

Here, E_a is the viscous flow activation energy, R is the universal gas constant, T is temperature, and τ_0 is the Arrhenius pre-factor. The calculated E_a for MyrAA-30-P-0.7 and MyrAA-30-T-0.7 were 67 and 91 kJ/mol respectively, which is consistent with the literature; the observed increase in the activation energy can be attributed to the different nature of the cross-linkers and the higher T_g of the latter network [6,34]. Figure 8.b compares the Arrhenius plots of MyrAA-30-T-0.7 (with 0.7:1 β-ketoester : NH_2 ratio) and MyrAA-30-T-1 (with 1:1 β-ketoester : NH_2 ratio). In the latter case, decreasing the concentration of amine groups to a balanced stoichiometric ratio increased the E_a to 105 kJ/mol. Typically, higher values of E_a indicate a higher energy barrier of bond exchange which leads to a rapid decrease of viscosity upon increasing temperature. In contrast, vitrimers with low E_a show less pronounced viscosity change with temperature alterations [13]. This trend agrees with the observed flow behavior of MyrAA-30-P-0.7, MyrAA-30-T-0.7, and MyrAA-30-T-1. A practical manifestation of this phenomenon can be utilized in the design of vitrimers with

enhanced dimensional stability at service temperatures and yet rapid viscosity decay with increasing temperatures which enables their fast processability [13,17,78]. Figure S17 compares the Arrhenius plots of MyrAA-30-P-0.7 and MyrAA-30-Long-P-30; a similar trend was observed with a slight increase of E_a value from 67 to 76 kJ/mol for the respective vitrimers.

Figure 9 shows the results of creep-recovery experiments for 5 different prepolymers vitrified with excess β-ketoester : amine ratio of 0.7:1. As the cross-linking density increased, the creep systematically decreased. Networks with copolymer having 10 and 20 mol% AAEMA content exhibited similar creep behavior with 2.8% and 2.6% shear strain at 300 s followed by some limited strain recovery of 27% and 28%, respectively. Further increasing the AAEMA content in the copolymer to 30 mol%, MyrAA-30-P-0.7, led to lower shear strain of 1.3% at 300 s which had 52% lower deformation compared to MyrAA-10-P-0.7. In addition, a higher creep recovery of 56% at 900 s was observed for MyrAA-30-P-0.7. At the 300 s point, the creep-recovery analysis of the MyrAA-30-Long-P-0.7, with $M_n \geq M_e$, revealed a lower deformation of about 49% compared to its counterpart, MyrAA-30-P-0.7, with a shorter backbone and $M_n < M_e$. Furthermore, we studied the influence of additional static cross-links in MyrAA-20-GMA-5-P-0.7. The dual cross-linked network showed the lowest deformation until 300 s combined with the highest creep recovery of 83% at 900 s. The high creep recovery in MyrAA-20-GMA-5-P-0.7 indicates that less permanent deformation had occurred in the sample. This can be credited to the presence of static cross-links which restricts network strand deformation [26,86]. The results of creep-recovery are in good agreement with those of stress-relaxation tests, showing that dimensional stability of the vitrimers can be tailored by cross-linking density, increasing primary chain length, and addition of physical or chemical, static cross-links [25,26,75,86].

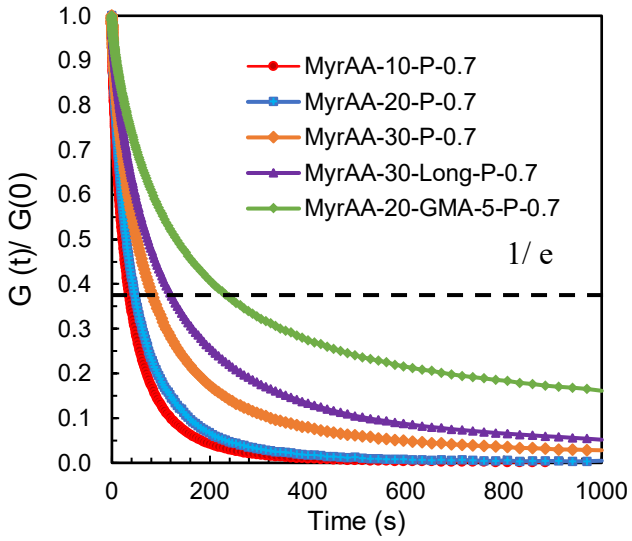

Figure. 7 Comparison of stress-relaxation behavior of various pre-polymers vitrified with an excess amount of Priamine (P-0.7) at 130 °C. Increasing AAEMA content and molecular weight of prepolymer ($M_n > M_e$) as well as incorporation of static cross-links systematically increased the relaxation time.

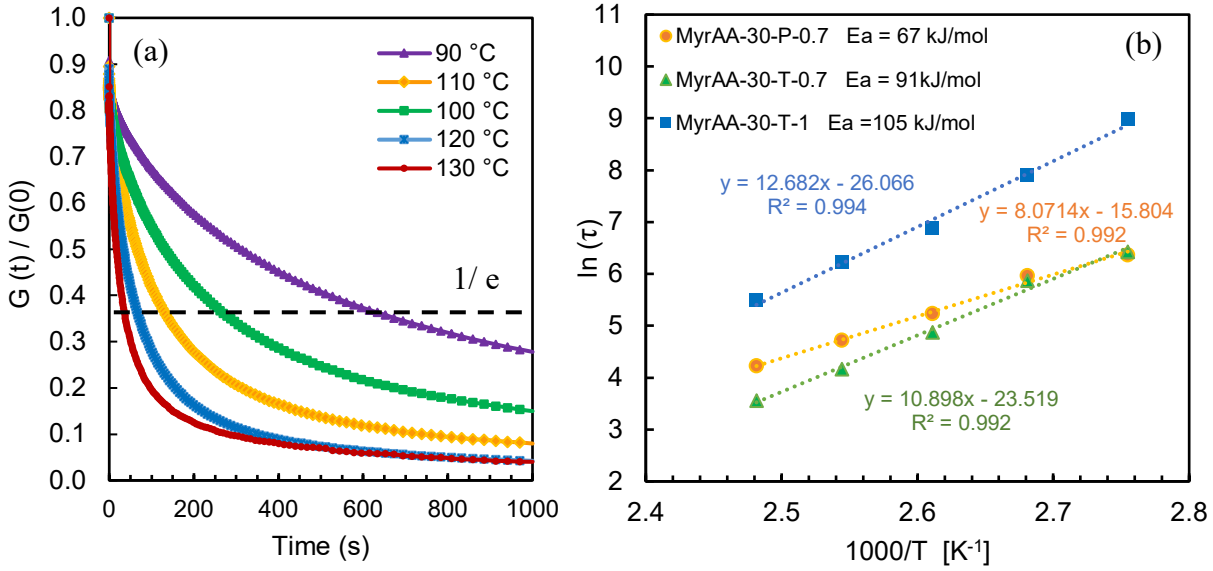

Figure 8. a) Comparison of stress-relaxation behavior of MyrAA-30-T-0.7 from 90 to 130 °C. **b)** Arrhenius relationship between relaxation time and temperature obtained from the stress relaxation experiment of the MyrAA-30-T-1 (with 1:1 β-ketoester : NH_2) and MyrAA-30-T-0.7 (with 0.7 : 1 β-ketoester : NH_2) vitrimers using stretched exponential decay fit.

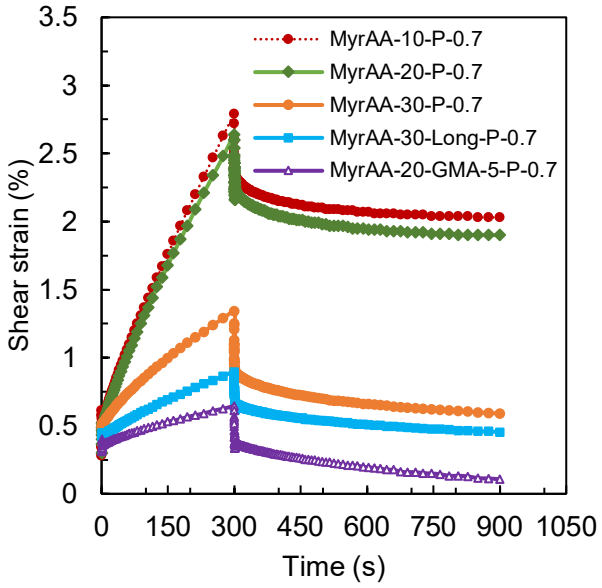

Figure 9. Creep-recovery data of various vitrimers cross-linked with excess Priamine (P-0.7). Creep was decreased by increasing the cross-linking density (AAEMA content), increasing the M_n of prepolymer (>M_e), and incorporating 5 mol% GMA to impart dual static and dynamic networks.

2.1. Recycling of vitrimers

Vitrimer reprocessability and ability to be remolded into new materials after curing is one of the most important properties of such polymer networks. This phenomenon is a direct consequence of the dynamic nature of the cross-links. Particularly, processability of vinylogous urethanes cured with TREN and Priamine were well-established by others [6,22,23,34,37]. Therefore, we mimicked similar recyclability tests by cutting the processed MyrAA-20-T-0.7 into small pieces and re-processing them via hot-pressing for 3 cycles. Figure 10 shows pictures of reprocessed and cut MyrAA-20-T-0.7 samples. We performed the compression molding at a relatively low temperature of 110 °C for 50 ± 5 min to minimize possible side reactions or degradation, and even though this temperature is lower than the values reported in the literature, well-formed samples were achieved. In addition, vitrified polymers showed high isothermal stability in a TGA test at 120 °C under nitrogen flow for 6 h (see Figure S11).

Figure 11 compares the thermomechanical and chemical properties of the original MyrAA-20-T-0.7 and those of the same sample after 3 recycling processes. ATR-FTIR spectra of the sample after each reprocessing cycle showed peaks attributed to the vinylogous urethanes at 1600 cm^{-1},

indicating N-H bending, and 1655 cm^{-1}, indicating C=C stretching, were retained and no other noticeable degradation was observed.

Thermal analyses by TGA and DSC shows that thermal properties of the vitrimer essentially stayed intact after reprocessing. The onset degradation at 360 °C with $T_{5\%}$ = 196 °C and T_g = -48 ± 1 °C was observed for the original and the recycled (3×) samples. DMTA analyses showed that the rubbery plateau was retained after 3× reprocessing with elastic modulus (G′) of 1.82 ± 0.5 MPa. Most importantly, the tensile properties remained intact after each processing cycle. Figure 11.d illustrates the stress-strain curves of the MyrAA-20-T-0.7 of the originally processed sample and its three consecutive reprocessed ones. Table 5 summarizes the results of tensile tests of reprocessed samples; respectively, average stress and elongation at break of 366 kPa and 21.7% were recorded for the (re)processed samples.

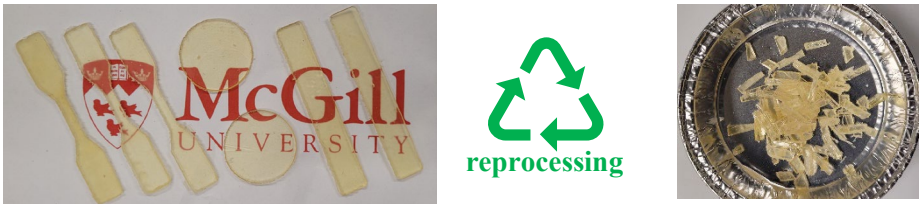

Figure 10. Reprocessing of poly(myrcene)-based vitrimers. Cured and processed samples were cut into small pieces and hot-pressed for 3 cycles.

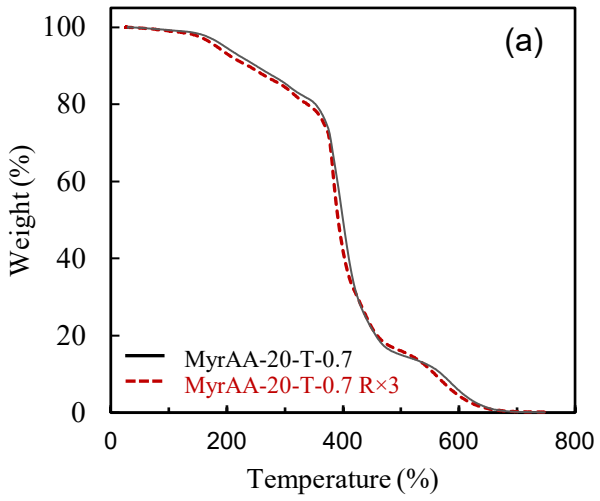
(a)
Weight (%)
Temperature (%)
MyrAA-20-T-0.7
MyrAA-20-T-0.7 R×3

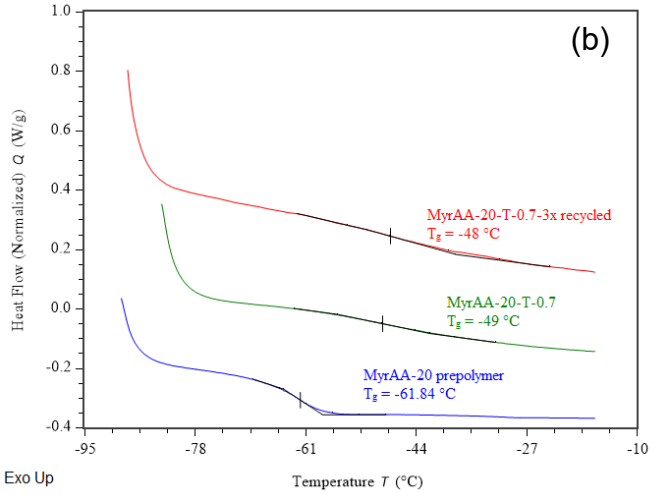
(b)
Heat Flow (Normalized) Q (W/g)
Temperature T (°C)
Exo Up
MyrAA-20-T-0.7-3x recycled
Tg = -48 °C
MyrAA-20-T-0.7
Tg = -49 °C
MyrAA-20 prepolymer
Tg = -61.84 °C

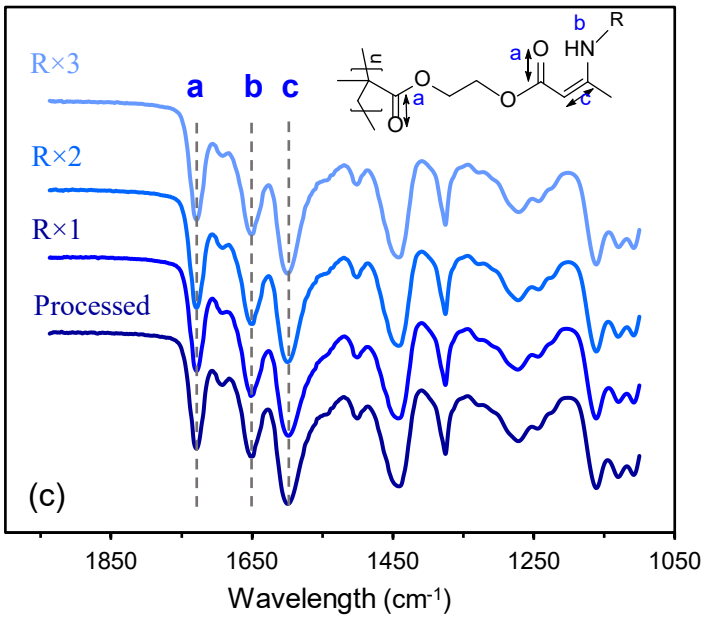
(c)
R×3
R×2
R×1
Processed
a b c
Wavelength (cm-1)

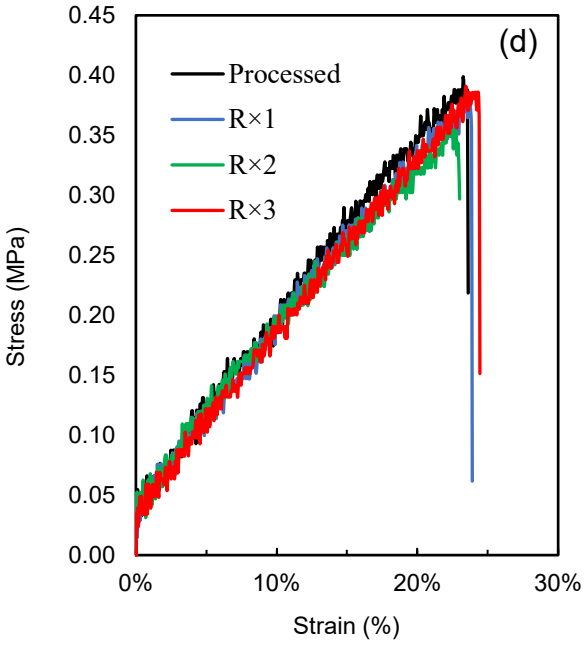
(d)
Processed
R×1
R×2
R×3
Stress (MPa)
Strain (%)

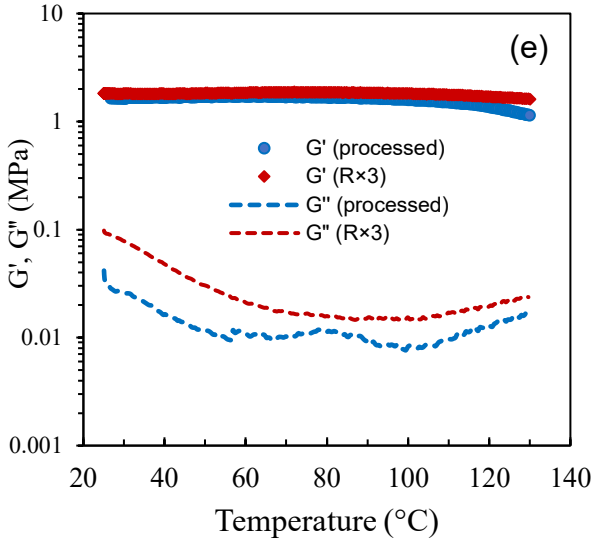
(e)
G' (processed)
G' (R×3)
G" (processed)
G" (R×3)
G', G" (MPa)
Temperature (°C)

Figure 11. Properties of reprocessed MyrAA-20-T-0.7 vitrimer after 3 cycles: a) TGA traces, thermal decomposition temperature with onset of 355 ± 5 °C did not change. b) DSC traces of MyrAA-20 prepolymer (blue line) with T_g of -61.8 °C, pristine processed Myr-AA-20-T-0.7 vitrimer (green line), and Myr-AA-20-T-0.7 vitrimer after 3 reprocessing cycles (red line); T_g was retained at ~ -48 ±1°C after vitrification and reprocessing. c) ATR-FTIR spectra, bands of N-H bending at 1600 cm^{-1} and C=C stretching at 1655 cm^{-1} corresponding to the vinylogous urethane cross-links retained. d) Stress-strain curves did not change e) Semi-logarithmic DMTA traces of originally processed vitrimer and after 3 reprocessing cycles (R×3), the rubbery plateau in elastic (G′) and loss (G″) was retained.

Table 5. Tensile properties of reprocessed MyrAA-20-T-0.7

MyrAA-30-T-0.7	Stress at break (kPa)	Strain at break (%)	Young's Modulus (MPa)
Original Processed	375.7 ± 22.7	22.1 ± 0.8	1.53 ± 0.04
Reprocessed ×1	362.6 ±29.0	22.6 ± 1.4	1.45 ± 0.02
Reprocessed ×2	348.3 ± 16.3	20.0 ± 2.1	1.54 ± 0.14
Reprocessed ×3	377.7 ± 52.4	22.3 ± 2.4	1.52 ± 0.09

An interesting consequence of dynamic cross-linking is the ability of different cured samples to be welded together without using significant pressure. Inspired by Liu et al., we performed a welding experiment by dabbing 2-3 drops of butylamine on top of two different rectangular samples each with a size and weight of about 1.5×1×0.1 cm (length×width×thickness) and 0.15 g respectively [84]. Afterwards, the samples were quickly combined and placed in an oven at 115 °C for 20 min. An empty NMR tube was placed on top of the samples to physically secure them, and no extra pressure was applied. The welded sample could resist up to 23.5 g, which is more than 60 times its weight. Control samples without any butylamine could not resist any external weight after a similar welding procedure was applied. Thus, it appears that butylamine caused welding by either solvent welding via swelling of the surfaces and/or possible liberation of some functional groups on the vitrimers and promotion of transamination between the two surfaces which led to a relatively fast and effective welding.

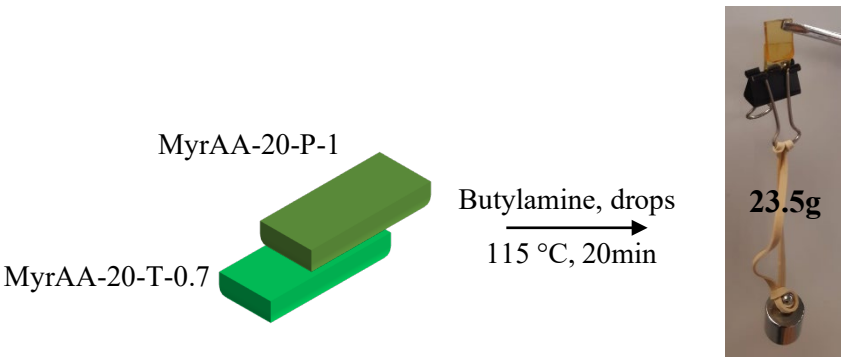

Figure 12. Welding of two different vitrimeric samples: MyrAA-20-P-1 and MyrAA20-T-0.7. Samples were dabbed with a few drops of butylamine at the interface and then heated for 20 min under no added pressure.

2.2. Shape memory

As mentioned in section 3.5, we originally synthesized the dual-functionalized MyrAA-20-GMA-5 prepolymer to impart both static and dynamic cross-links with the goal of reducing creep. Additionally, we hypothesized that shape memory effects can be seen in this material as static epoxy-amine cross-links can "memorize" the permanent shape of the vitrimer while the dynamic vinylogous urethane can retain the temporary shape. Therefore, we first vitrified the sample in a rectangular mold, i.e., the permanent shape. Afterwards, the sample was heated and carefully bent and reshaped, the temporary shape, and kept in an oven at 110 °C under vacuum for 1 h. This was followed by cooling of the sample under stress. The resulting sample's shape, Figure 13.b, was temporarily stable, at least for 48 h, until it was heated again in an oven at 120 °C. The full shape recovery was achieved in about 4 h. While good shape fixity and shape recovery ratio was observed, the rate of shape recovery was slow. These results are in line with the observed slower stress-relaxation, Figure 7, and full creep-recovery, Figure 9, of MyrAA-20-GMA-5. Although a simple shape recovery is reported, this initial exploration combining shape recovery with dynamic

networks was very promising and more in-depth studies on exploring the interplay of the chemistries to tailor recovery times are underway.

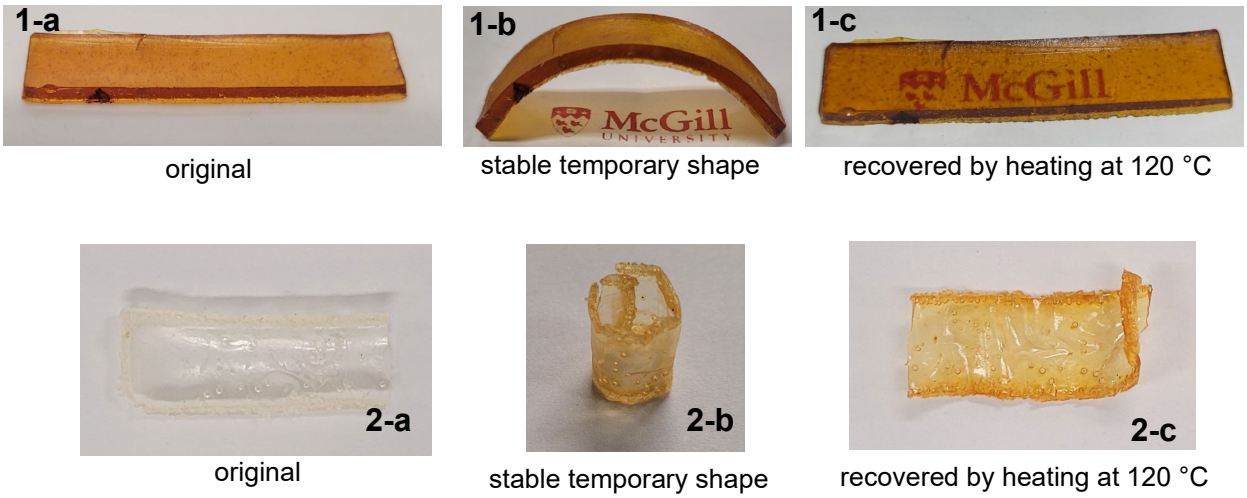

Figure 13. Shape memory effect of 2 different MyrAA-18-GMA-8-P-0.7 samples. a) original shape was formed after vitrification as described in section 2.3 b) temporary shape was formed after heating to 110 °C and cooling under stress; the shape was stable at room temperature for at least 24hr c) recovery of the original shape by reheating to 120 °C for 4 h.

3. Conclusions

Development of elastomers from renewable feedstocks with enhanced recyclability is a step forward towards a more sustainable rubber industry. We have demonstrated a straightforward approach to synthesize bio-based vitrimers using commercially available and relatively inexpensive myrcene with catalyst-free vinylogous urethane chemistry for the first time. Statistical prepolymers of Myr and AAEMA were prepared in a controlled fashion using NMP and afterwards cross-linked with biobased Priamine or TREN via solution casting and compression molding. The final mechanical and rheological properties of the networks could be effectively tailored by

changing the prepolymers' composition, molecular weight, and the nature and ratio of the cross-linkers. The rubbery networks exhibited effective reprocessability by mechanical grinding and hot pressing at 110 °C in less than 60 min for at least 3 cycles. ATR-FTIR confirmed retention of the network while no change in the T_g, onset of decomposition, storage modulus as well as elongation and stress at break was observed after reprocessing. Although vitrimer-like insolubility of the networks in different solvents was confirmed, prepolymers could be chemically recovered by addition of excess monofunctional amines at 110 °C without degradation, confirmed by GPC. Also, Myr-based vitrimers could be welded to each other by using a few drops of n-butyl amine at 115 °C in 20 min. Increasing the prepolymer's molecular weight beyond its entanglement limit ($M_n > M_e$) led to decreased creep. In addition, dual networks with static and dynamic cross-links were formed by incorporation of 5 mol% epoxy-based GMA in the prepolymer. The resulting network exhibited significant reduction in creep in addition to shape memory effects.

Adopting vitrimer chemistry is a versatile and yet simple tool in tailoring the thermomechanical properties of poly(Myr) with excellent reprocessability. We envision that this approach can be used as a platform to develop customized recyclable biobased elastomers with applications in rubbers, smart materials, wearable electronics, to name but a few.

4. Associated Information

Synthetic route, photographs of vitrification steps, ^{1}H NMR of prepolymers, GPC traces, DSC, calculation of solubility parameters, TGA, swelling tests, rheological data, ATR-FTIR spectra are found in the Supporting Information.

5. Acknowledgments

This research was supported by the Natural Sciences and Engineering Research Council of

Canada (NSERC, Discovery Grant RGPIN-2019-05948). Authors would like to thank Alexander Graham Bell Canada Graduate Scholarship (FA) for financial support and the Centre Québécois sur les Matériaux Fonctionnels (CQMF) and McGill Institute for Advanced Materials (MIAM) for the use of the DSC and TGA. We also thank Stephen Carson from Arkema for his help in procuring the BlocBuilder MA.

6. References

(1) Borrelle, S. B.; Ringma, J.; Law, K. L.; Monnahan, C. C.; Lebreton, L.; McGivern, A.; Murphy, E.; Jambeck, J.; Leonard, G. H.; Hilleary, M. A.; Eriksen, M.; Possingham, H. P.; de Frond, H.; Gerber, L. R.; Polidoro, B.; Tahir, A.; Bernard, M.; Mallos, N.; Barnes, M.; Rochman, C. M. Predicted Growth in Plastic Waste Exceeds Efforts to Mitigate Plastic Pollution. *Science (1979)* **2020**, *369* (6510), 1515–1518. https://doi.org/10.1126/science.aba3656.

(2) Cywar, R. M.; Rorrer, N. A.; Hoyt, C. B.; Beckham, G. T.; Chen, E. Y.-X. Bio-Based Polymers with Performance-Advantaged Properties. *Nat Rev Mater* **2021**, *7* (2), 83–103. https://doi.org/10.1038/s41578-021-00363-3.

(3) Younes, G. R.; Marić, M. Bio-Based Thermoplastic Polyhydroxyurethanes Synthesized from the Terpolymerization of a Dicarbonate and Two Diamines: Design, Rheology, and Application in Melt Blending. *Macromolecules* **2021**, *54* (21), 10189–10202. https://doi.org/10.1021/acs.macromol.1c01640.

(4) Brencio, C.; Maruzzi, M.; Manzolini, G.; Gallucci, F. Butadiene Production in Membrane Reactors: A Techno-Economic Analysis. *Int J Hydrogen Energy* **2022**, *47* (50), 21375–21390. https://doi.org/10.1016/J.IJHYDENE.2022.04.259.

(5) Imbernon, L.; Oikonomou, E. K.; Norvez, S.; Leibler, L. Chemically Crosslinked yet Reprocessable Epoxidized Natural Rubber via Thermo-Activated Disulfide Rearrangements. *Polym. Chem* **2015**, *6*, 4271. https://doi.org/10.1039/c5py00459d.

(6) Denissen, W.; Droesbeke, M.; Nicola, R.; Leibler, L.; Winne, J. M.; du Prez, F. E. Chemical Control of the Viscoelastic Properties of Vinylogous Urethane Vitrimers. *Nature Communications 2017 8:1* **2017**, *8* (1), 1–7. https://doi.org/10.1038/ncomms14857.

(7) Lessard, J. J.; Scheutz, G. M.; Hughes, R. W.; Sumerlin, B. S. Polystyrene-Based Vitrimers: Inexpensive and Recyclable Thermosets. *ACS Appl Polym Mater* **2020**, *2* (8), 3044–3048. https://doi.org/10.1021/acsapm.0c00523.

(8) Wemyss, A. M.; Bowen, C.; Plesse, C.; Vancaeyzeele, C.; Nguyen, G. T. M.; Vidal, F.; Wan, C. Dynamic Crosslinked Rubbers for a Green Future: A Material Perspective. *Materials Science and Engineering: R: Reports* **2020**, *141*, 100561. https://doi.org/10.1016/j.mser.2020.100561.

(9) Bowman, C. N.; Kloxin, C. J. Covalent Adaptable Networks: Reversible Bond Structures Incorporated in Polymer Networks. *Angewandte Chemie International Edition* **2012**, *51* (18), 4272–4274. https://doi.org/10.1002/anie.201200708.

(10) Kloxin, C. J.; Scott, T. F.; Adzima, B. J.; Bowman, C. N. Covalent Adaptable Networks (CANs): A Unique Paradigm in Cross-Linked Polymers. *Macromolecules* **2010**, *43*, 2643. https://doi.org/10.1021/ma902596s.

(11) Adzima, B. J.; Aguirre, H. A.; Kloxin, C. J.; Scott, T. F.; Bowman, C. N. Rheological and Chemical Analysis of Reverse Gelation in a Covalently Cross-Linked Diels−Alder Polymer Network. *Macromolecules* **2008**, *41* (23), 9112–9117. https://doi.org/10.1021/ma801863d.

(12) Wang, S.; Urban, M. W. Self-Healing Polymers. *Nat Rev Mater* **2020**, *5* (8), 562–583. https://doi.org/10.1038/s41578-020-0202-4.

(13) Scheutz, G. M.; Lessard, J. J.; Sims, M. B.; Sumerlin, B. S. Adaptable Crosslinks in Polymeric Materials: Resolving the Intersection of Thermoplastics and Thermosets. *J Am Chem Soc* **2019**, *141* (41), 16181–16196. https://doi.org/10.1021/jacs.9b07922.

(14) Montarnal, D.; Capelot, M.; Tournilhac, F.; Leibler, L. Silica-Like Malleable Materials from Permanent Organic Networks. *Science (1979)* **2011**, *334* (6058), 965–968. https://doi.org/10.1126/science.1212648.

(15) Winne, J. M.; Leibler, L.; du Prez, F. E. Dynamic Covalent Chemistry in Polymer Networks: A Mechanistic Perspective. *Polymer Chemistry*. Royal Society of Chemistry December 7, 2019, pp 6091–6108. https://doi.org/10.1039/c9py01260e.

(16) Denissen, W.; Winne, J. M.; Du Prez, F. E. Vitrimers: Permanent Organic Networks with Glass-like Fluidity. *Chem Sci* **2016**, *7* (1), 30–38. https://doi.org/10.1039/C5SC02223A.

(17) Röttger, M.; Domenech, T.; van der Weegen, R.; Breuillac, A.; Nicolaÿ, R.; Leibler, L. High-Performance Vitrimers from Commodity Thermoplastics through Dioxaborolane

Metathesis. *Science (1979)* **2017**, *356* (6333), 62–65. https://doi.org/10.1126/science.aah5281.

(18) Nishimura, Y.; Chung, J.; Muradyan, H.; Guan, Z. Silyl Ether as a Robust and Thermally Stable Dynamic Covalent Motif for Malleable Polymer Design. *J Am Chem Soc* **2017**, *139* (42), 14881–14884. https://doi.org/10.1021/jacs.7b08826.

(19) Zheng, P.; McCarthy, T. J. A Surprise from 1954: Siloxane Equilibration Is a Simple, Robust, and Obvious Polymer Self-Healing Mechanism. *J Am Chem Soc* **2012**, *134* (4), 2024–2027. https://doi.org/10.1021/ja2113257.

(20) Taynton, P.; Yu, K.; Shoemaker, R. K.; Jin, Y.; Qi, H. J.; Zhang, W. Heat- or Water-Driven Malleability in a Highly Recyclable Covalent Network Polymer. *Advanced Materials* **2014**, *26* (23), 3938–3942. https://doi.org/10.1002/adma.201400317.

(21) Schoustra, S. K.; de Heer Kloots, M. H. P.; Posthuma, J.; van Doorn, D.; Dijksman, J. A.; Smulders, M. M. J. Raman Spectroscopy Reveals Phase Separation in Imine-Based Covalent Adaptable Networks. *Macromolecules* **2022**, *55* (23), 10341–10355. https://doi.org/10.1021/acs.macromol.2c01595.

(22) Denissen, W.; Rivero, G.; Nicolaÿ, R.; Leibler, L.; Winne, J. M.; du Prez, F. E. Vinylogous Urethane Vitrimers. *Adv Funct Mater* **2015**, *25* (16), 2451–2457. https://doi.org/10.1002/ADFM.201404553.

(23) Hajiali, F.; Tajbakhsh, S.; Marić, M. Thermally Reprocessable Bio-Based Polymethacrylate Vitrimers and Nanocomposites. *Polymer* **2021**, *212*, 123126. https://doi.org/10.1016/j.polymer.2020.123126.

(24) Pepels, M.; Filot, I.; Klumperman, B.; Goossens, H. Self-Healing Systems Based on Disulfide-Thiol Exchange Reactions. *Polym Chem* **2013**, *4* (18), 4955–4965. https://doi.org/10.1039/c3py00087g.

(25) Breuillac, A.; Kassalias, A.; Nicolaÿ, R. Polybutadiene Vitrimers Based on Dioxaborolane Chemistry and Dual Networks with Static and Dynamic Cross-Links. *Macromolecules* **2019**, *52* (18), 7102–7113. https://doi.org/10.1021/acs.macromol.9b01288.

(26) Cash, J. J.; Kubo, T.; Dobbins, D. J.; Sumerlin, B. S. Maximizing the Symbiosis of Static and Dynamic Bonds in Self-Healing Boronic Ester Networks. *Polym Chem* **2018**, *9* (15), 2011–2020. https://doi.org/10.1039/c8py00123e.

(27) Tajbakhsh, S.; Hajiali, F.; Guinan, K.; Marić, M. Highly Reprocessable, Room Temperature Self-Healable Bio-Based Materials with Boronic-Ester Dynamic Cross-Linking. *React Funct Polym* **2021**, *158*, 104794. https://doi.org/10.1016/j.reactfunctpolym.2020.104794.

(28) Fortman, D. J.; Brutman, J. P.; Cramer, C. J.; Hillmyer, M. A.; Dichtel, W. R. Mechanically Activated, Catalyst-Free Polyhydroxyurethane Vitrimers. *J. Am. Chem. Soc* **2015**, *137*. https://doi.org/10.1021/jacs.5b08084.

(29) Yu, S.; Wu, S.; Zhang, C.; Tang, Z.; Luo, Y.; Guo, B.; Zhang, L. Catalyst-Free Metathesis of Cyclic Acetals and Spirocyclic Acetal Covalent Adaptable Networks. *ACS Macro Lett* **2020**, *9* (8), 1143–1148. https://doi.org/10.1021/acsmacrolett.0c00527.

(30) Ahmadi, M.; Hanifpour, A.; Ghiassinejad, S.; van Ruymbeke, E. Polyolefins Vitrimers: Design Principles and Applications. *Chemistry of Materials* **2022**, *34* (23), 10249–10271. https://doi.org/10.1021/acs.chemmater.2c02853.

(31) Zheng, J.; Png, Z. M.; Ng, S. H.; Tham, G. X.; Ye, E.; Goh, S. S.; Loh, X. J.; Li, Z. Vitrimers: Current Research Trends and Their Emerging Applications. *Materials Today* **2021**. https://doi.org/10.1016/j.mattod.2021.07.003.

(32) van Zee, N. J.; Nicolaÿ, R. Vitrimers: Permanently Crosslinked Polymers with Dynamic Network Topology. *Prog Polym Sci* **2020**, *104*, 101233. https://doi.org/10.1016/j.progpolymsci.2020.101233.

(33) Porath, L.; Soman, B.; Jing, B. B.; Evans, C. M. Vitrimers: Using Dynamic Associative Bonds to Control Viscoelasticity, Assembly, and Functionality in Polymer Networks. *ACS Macro Lett* **2022**, *11* (4), 475–483. https://doi.org/10.1021/acsmacrolett.2c00038.

(34) Lessard, J. J.; Garcia, L. F.; Easterling, C. P.; Sims, M. B.; Bentz, K. C.; Arencibia, S.; Savin, D. A.; Sumerlin, B. S. Catalyst-Free Vitrimers from Vinyl Polymers. *Macromolecules* **2019**, *52* (5), 2105–2111. https://doi.org/https://pubs.acs.org/doi/abs/10.1021/acs.macromol.8b02477.

(35) Perego, A.; Khabaz, F. Creep and Recovery Behavior of Vitrimers with Fast Bond Exchange Rate. *Macromol Rapid Commun* **2023**, *44* (1), 2200313. https://doi.org/10.1002/marc.202200313.

(36) Lessard, J. J.; Scheutz, G. M.; Sung, S. H.; Lantz, K. A.; Epps, T. H.; Sumerlin, B. S. Block Copolymer Vitrimers. *J Am Chem Soc* **2020**, *142* (1). https://doi.org/10.1021/jacs.9b10360.

(37) Ishibashi, J. S. A.; Pierce, I. C.; Chang, A. B.; Zografos, A.; El-Zaatari, B. M.; Fang, Y.; Weigand, S. J.; Bates, F. S.; Kalow, J. A. Mechanical and Structural Consequences of Associative Dynamic Cross-Linking in Acrylic Diblock Copolymers. *Macromolecules* **2021**, *54* (9), 3972–3986. https://doi.org/10.1021/acs.macromol.0c02744.

(38) Van Lijsebetten, F.; De Bruycker, K.; Spiesschaert, Y.; Winne, J. M.; Du Prez, F. E. Suppressing Creep and Promoting Fast Reprocessing of Vitrimers with Reversibly Trapped Amines. *Angewandte Chemie International Edition* **2022**, *61* (9), e202113872. https://doi.org/10.1002/anie.202113872.

(39) Chuanbing Tang; Chang Y. Ryu. *Sustainable Polymers from Biomass*; Tang, C., Ryu, C. Y., Eds.; Wiley-VCH Verlag GmbH & Co. KGaA: Weinheim, Germany, 2017. https://doi.org/10.1002/9783527340200.

(40) Bauer, N.; Brunke, J.; Kali, G. Controlled Radical Polymerization of Myrcene in Bulk: Mapping the Effect of Conditions on the System. *ACS Sustain Chem Eng* **2017**, *5* (11), 10084–10092. https://doi.org/10.1021/acssuschemeng.7b02091.

(41) Sarkar, P.; Bhowmick, A. K. Terpene Based Sustainable Elastomer for Low Rolling Resistance and Improved Wet Grip Application: Synthesis, Characterization and Properties of Poly(Styrene-Co-Myrcene). *ACS Sustain Chem Eng* **2016**, *4* (10), 5462–5474. https://doi.org/10.1021/ACSSUSCHEMENG.6B01038

(42) Luk, S. B.; Azevedo, L. A.; Maric, M. Reversible Deactivation Radical Polymerization of Bio-Based Dienes. *React Funct Polym* **2021**, *162*, 104871. https://doi.org/10.1016/j.reactfunctpolym.2021.104871.

(43) Magaña, I.; López, R.; Enríquez-Medrano, F. J.; Kumar, S.; Aguilar-Sanchez, A.; Handa, R.; Díaz de León, R.; Valencia, L. Bioelastomers: Current State of Development. *J Mater Chem A Mater* **2022**, *10* (10), 5019–5043. https://doi.org/10.1039/D1TA09404A.

(44) Luk, S. B.; Métafiot, A.; Morize, J.; Edeh, E.; Marić, M. Hydrogenation of Poly(Myrcene) and Poly(Farnesene) Using Diimide Reduction at Ambient Pressure. *Journal of Polymer Science* **2021**, *59* (19), 2140–2153. https://doi.org/10.1002/POL.20210479.

(45) Behr, A.; Johnen, L. Myrcene as a Natural Base Chemical in Sustainable Chemistry: A Critical Review. *ChemSusChem* **2009**, *2* (12), 1072–1095. https://doi.org/10.1002/CSSC.200900186.

(46) Halloran, M. W.; Nicell, J. A.; Leask, R. L.; Marić, M. Toughening Poly(Lactide) with Bio-Based Poly(Farnesene) Elastomers. *ACS Appl Polym Mater* **2022**, *4* (8), 6276–6287. https://doi.org/10.1021/acsapm.2c01183.

(47) Métafiot, A.; Kanawati, Y.; Gérard, J. F.; Defoort, B.; Marić, M. Synthesis of β-Myrcene-Based Polymers and Styrene Block and Statistical Copolymers by SG1 Nitroxide-Mediated Controlled Radical Polymerization. *Macromolecules* **2017**, *50* (8), 3101–3120. https://doi.org/10.1021/ACS.MACROMOL.6B02675

(48) Wahlen, C.; Frey, H. Anionic Polymerization of Terpene Monomers: New Options for Bio-Based Thermoplastic Elastomers. *Macromolecules* **2021**, *54* (16), 7323–7336. https://doi.org/10.1021/acs.macromol.1c00770.

(49) Sahu, P.; Bhowmick, A. K.; Kali, G. Terpene Based Elastomers: Synthesis, Properties, and Applications. *Processes* **2020**, *8* (5), 553. https://doi.org/10.3390/pr8050553.

(50) Zhang, S.; Han, L.; Ma, H.; Liu, P.; Shen, H.; Lei, L.; Li, C.; Yang, L.; Li, Y. Investigation on Synthesis and Application Performance of Elastomers with Biogenic Myrcene. *Ind Eng Chem Res* **2019**, *58* (28), 12845–12853. https://doi.org/10.1021/acs.iecr.9b02010.

(51) Sahu, P.; Bhowmick, A. K.; Kali, G. Terpene Based Elastomers: Synthesis, Properties, and Applications. *Processes* **2020**, *8* (5), 553. https://doi.org/10.3390/pr8050553.

(52) Métafiot, A.; Gagnon, L.; Pruvost, S.; Hubert, P.; Gérard, J.-F.; Defoort, B.; Marić, M. β-Myrcene/Isobornyl Methacrylate SG1 Nitroxide-Mediated Controlled Radical Polymerization: Synthesis and Characterization of Gradient, Diblock and Triblock Copolymers. *RSC Adv* **2019**, *9* (6), 3377–3395. https://doi.org/10.1039/C8RA09192G.

(53) Sarkar, P.; Bhowmick, A. K. Synthesis, Characterization and Properties of a Bio-Based Elastomer: Polymyrcene. *RSC Adv.* **2014**, *4* (106), 61343–61354. https://doi.org/10.1039/C4RA09475A.

(54) Kitphaitun, S.; Chaimongkolkunasin, S.; Manit, J.; Makino, R.; Kadota, J.; Hirano, H.; Nomura, K. Ethylene/Myrcene Copolymers as New Bio-Based Elastomers Prepared by Coordination Polymerization Using Titanium Catalysts. *Macromolecules* **2021**, *54* (21), 10049–10058. https://doi.org/10.1021/acs.macromol.1c01878.

(55) Sarkar, P.; Bhowmick, A. K. Terpene Based Sustainable Elastomer for Low Rolling Resistance and Improved Wet Grip Application: Synthesis, Characterization and Properties

of Poly(Styrene-Co-Myrcene). *ACS Sustain Chem Eng* **2016**, *4* (10), 5462–5474. https://doi.org/10.1021/acssuschemeng.6b01038.

(56) Sahu, P.; Bhowmick, A. K. Sustainable Self-Healing Elastomers with Thermoreversible Network Derived from Biomass via Emulsion Polymerization. *J Polym Sci A Polym Chem* **2019**, *57* (6), 738–751. https://doi.org/10.1002/pola.29320.

(57) Luo, W.; Yang, P.; Gan, Q.; Zhao, Z.; Tang, F.; Xu, Y.; Jia, X.; Gong, D. Reversible Addition–Fragmentation Chain Transfer Polymerization of Myrcene Derivatives: An Efficient Access to Fully Bio-Sourced Functional Elastomers with Recyclable, Shape Memory and Self-Healing Properties. *Polym Chem* **2021**, *12* (25), 3677–3687. https://doi.org/10.1039/D1PY00549A.

(58) Li, P.; Hao, C.; Wang, H.; He, T.; Shu, T.; Li, C.; Yu, L.; Yan, N. Eco-Friendly Recyclable High Performance Ramie Yarn Reinforced Polyimine Vitrimer Composites. *Chemical Engineering Journal* **2023**, *457*, 141341. https://doi.org/10.1016/j.cej.2023.141341.

(59) Kölsch, J. C.; Berač, C. M.; Lossada, F.; Stach, O. S.; Seiffert, S.; Walther, A.; Besenius, P. Recyclable Vitrimers from Biogenic Poly(Itaconate) Elastomers. *Macromolecules* **2022**, *55* (18), 8032–8039. https://doi.org/10.1021/acs.macromol.2c00825.

(60) Feng, Z.; Hu, J.; Zuo, H.; Ning, N.; Zhang, L.; Yu, B.; Tian, M. Photothermal-Induced Self-Healable and Reconfigurable Shape Memory Bio-Based Elastomer with Recyclable Ability. *ACS Appl Mater Interfaces* **2019**, *11* (1), 1469–1479. https://doi.org/10.1021/acsami.8b18002.

(61) Liu, W.; Huang, J.; Gong, Z.; Fan, J.; Chen, Y. Healable, Recyclable and Mechanically Robust Elastomers with Multiple Dynamic Cross-Linking Bonds. *Polymer (Guildf)* **2022**, *252*, 124900. https://doi.org/10.1016/J.POLYMER.2022.124900.

(62) Vinas, J.; Chagneux, N.; Gigmes, D.; Trimaille, T.; Favier, A.; Bertin, D. SG1-Based Alkoxyamine Bearing a N-Succinimidyl Ester: A Versatile Tool for Advanced Polymer Synthesis. *Polymer (Guildf)* **2008**, *49* (17), 3639–3647. https://doi.org/10.1016/j.polymer.2008.06.017.

(63) Moayeri, A.; Lessard, B.; Maric, M. Nitroxide Mediated Controlled Synthesis of Glycidyl Methacrylate-Rich Copolymers Enabled by SG1-Based Alkoxyamines Bearing Succinimidyl Ester Groups. *Polym Chem* **2011**, *2* (9), 2084. https://doi.org/10.1039/c1py00190f.

(64) Luk, S. B.; Marić, M. Nitroxide-Mediated Polymerization of Bio-Based Farnesene with a Functionalized Methacrylate. *Macromol React Eng* **2019**, *13* (3), 1800080. https://doi.org/10.1002/mren.201800080.

(65) Pablo-Morales, Á.; Treviño, M. E.; Saldívar-Guerra, E. Toward Bio-Sourced Elastomers with Reactive/Polar Groups. Myrcene – Glycidyl Methacrylate Copolymerization: Reactivity Ratios, Properties, and Preliminary RAFT Emulsion Polymerization. *Macromol React Eng* **2022**, *16* (3), 2200007. https://doi.org/10.1002/mren.202200007.

(66) Hilschmann, J.; Kali, G. Bio-Based Polymyrcene with Highly Ordered Structure via Solvent Free Controlled Radical Polymerization. *Eur Polym J* **2015**, *73*, 363–373. https://doi.org/10.1016/J.EURPOLYMJ.2015.10.021.

(67) Métafiot, A.; Gérard, J. F.; Defoort, B.; Marić, M. Synthesis of β-Myrcene/Glycidyl Methacrylate Statistical and Amphiphilic Diblock Copolymers by SG1 Nitroxide-Mediated Controlled Radical Polymerization. *J Polym Sci A Polym Chem* **2018**, *56* (8), 860–878. https://doi.org/10.1002/POLA.28963.

(68) Nicolas, J.; Guillaneuf, Y.; Bertin, D.; Gigmes, D.; Charleux, B. Nitroxide-Mediated Polymerization. In *Polymer Science: A Comprehensive Reference, 10 Volume Set*; Elsevier, 2012; Vol. 3, pp 277–350. https://doi.org/10.1016/B978-0-444-53349-4.00069-8.

(69) Noppalit, S.; Simula, A.; Billon, L.; Asua, J. M. On the Nitroxide Mediated Polymerization of Methacrylates Derived from Bio-Sourced Terpenes in Miniemulsion, a Step towards Sustainable Products. *Polym Chem* **2020**, *11* (6), 1151–1160. https://doi.org/10.1039/C9PY01667H.

(70) Lamontagne, H. R.; Lessard, B. H. Nitroxide-Mediated Polymerization: A Versatile Tool for the Engineering of Next Generation Materials. *ACS Appl Polym Mater* **2020**, *2* (12), 5327–5344. https://doi.org/10.1021/acsapm.0c00888.

(71) Likhtenshtein, G. I. Nitroxide-Mediated Polymerization. In *Nitroxides*; Springer, 2020; pp 161–186.

(72) Braunecker, W. A.; Matyjaszewski, K. Controlled/Living Radical Polymerization: Features, Developments, and Perspectives. *Prog Polym Sci* **2007**, *32* (1), 93–146. https://doi.org/10.1016/j.progpolymsci.2006.11.002.

(73) Iacob, C.; Heck, M.; Wilhelm, M. Molecular Dynamics of Polymyrcene: Rheology and Broadband Dielectric Spectroscopy on a Stockmayer Type A Polymer. *Macromolecules* **2023**, *56* (1), 188–197. https://doi.org/10.1021/acs.macromol.2c01884.

(74) Sperling, L. H. *Introduction to Physical Polymer Science*, 4th ed.; Wiley, 2005. https://doi.org/10.1002/0471757128.

(75) Lessard, J. J.; Stewart, K. A.; Sumerlin, B. S. Controlling Dynamics of Associative Networks through Primary Chain Length. *Macromolecules* **2022**, *55* (22), 10052–10061. https://doi.org/10.1021/acs.macromol.2c01909.

(76) van Lijsebetten, F.; de Bruycker, K.; Winne, J. M.; du Prez, F. E. Masked Primary Amines for a Controlled Plastic Flow of Vitrimers. *ACS Macro Lett* **2022**, *11* (7), 919–924. https://doi.org/10.1021/acsmacrolett.2c00255.

(77) Montarnal, D.; Capelot, M.; Tournilhac, F.; Leibler, L. Silica-like Malleable Materials from Permanent Organic Networks. *Science (1979)* **2011**, *334* (6058), 965–968. https://doi.org/10.1126/SCIENCE.1212648/

(78) Winne, J. M.; Leibler, L.; du Prez, F. E. Dynamic Covalent Chemistry in Polymer Networks: A Mechanistic Perspective. *Polym Chem* **2019**, *10* (45), 6091–6108. https://doi.org/10.1039/C9PY01260E.

(79) Luk, S. B.; Maric, M. Farnesene and Norbornenyl Methacrylate Block Copolymers: Application of Thiol-Ene Clicking to Improve Thermal and Mechanical Properties. *Polymer (Guildf)* **2021**, *230*, 124106. https://doi.org/10.1016/j.polymer.2021.124106.

(80) Flory, P. J. *Principles of Polymer Chemistry*; Cornell University Press: Ithaca, N.Y., 1953.

(81) Lodge, T. P.; Hiemenz, P. C. *Polymer Chemistry*, Third edition.; CRC Press, 2020. https://doi.org/10.1201/9780429190810.

(82) Flory, P. J. Statistical Mechanics of Swelling of Network Structures. *J Chem Phys* **1950**, *18* (1), 108–111. https://doi.org/10.1063/1.1747424.

(83) van Krevelen, D. W.; te Nijenhuis, K. Cohesive Properties and Solubility. *Properties of Polymers* **2009**, 189–227. https://doi.org/10.1016/B978-0-08-054819-7.00007-8.

(84) Liu, Z.; Zhang, C.; Shi, Z.; Yin, J.; Tian, M. Tailoring Vinylogous Urethane Chemistry for the Cross-Linked Polybutadiene: Wide Freedom Design, Multiple Recycling Methods, Good Shape Memory Behavior. *Polymer (Guildf)* **2018**, *148*, 202–210. https://doi.org/10.1016/j.polymer.2018.06.042.

(85) Self, J. L.; Dolinski, N. D.; Zayas, M. S.; Read De Alaniz, J.; Bates, C. M. Brønsted-Acid-Catalyzed Exchange in Polyester Dynamic Covalent Networks. *ACS Macro Lett* **2018**, *7*, 821. https://doi.org/10.1021/acsmacrolett.8b00370.

(86) Li, L.; Chen, X.; Jin, K.; Torkelson, J. M. Vitrimers Designed Both to Strongly Suppress Creep and to Recover Original Cross-Link Density after Reprocessing: Quantitative Theory and Experiments. *Macromolecules* **2018**, *51* (15), 5537–5546. https://doi.org/https://pubs.acs.org/doi/abs/10.1021/acs.macromol.8b00922.